A Post-2013 Drop-off in Total Ozone at Half of Global Ozonesonde Stations: ECC Instrument Artifacts?

Ryan Michael Stauffer[1,1,1], Anne M. Thompson[2,2,2], Debra E Kollonige[3,3,3], Jacquelyn Cecile Witte[4,4,4], David W. Tarasick[5,5,5], Jonathan Davies[6,6,6], Holger Voemel[7,7,7], Gary A. Morris[8,8,8], Roeland VanMalderen[9,9,9], Bryan J. J. Johnson[10,10,10], Richard Querel[11,11,11], Henry B Selkirk[12,12,12], Rene Stuebi[13,13,13], and Herman G.J. Smit[14,14,14]

[1]NASA Goddard Space Flight Center
[2]NASA-GODDARD
[3]University of Maryland - Earth System Science Interdisciplinary Center
[4]National Center for Atmospheric Research
[5]Environment and Climate Change Canada
[6]Environment Canada
[7]Unknown
[8]St. Edward's University
[9]Royal Meteorological Institute of Belgium
[10]NOAA ESRL
[11]National Institute of Water & Atmospheric Research (NIWA)
[12]Goddard Earth Sciences and Technology Center, University of Maryland, Baltimore County
[13]MeteoSwiss
[14]Forschungszentrum Juelich, Germany

November 30, 2022

Abstract

An international effort to improve ozonesonde data quality and to reevaluate historical records has made significant improvements in the accuracy of global network data. However, between 2014 and 2016, ozonesonde total column ozone (TCO; O3) at 14 of 37 regularly reporting stations exhibited a sudden drop-off relative to satellite measurements. The ozonesonde TCO drop is 3-7 % compared to satellite and ground-based TCO, and 5-10 % or more compared to satellite stratospheric O3 profiles, compromising the use of recent data for trends, although they remain reliable for other uses. Hardware changes in the ozonesonde instrument are likely a major factor in the O3 drop-off, but no single property of the ozonesonde explains the findings. The bias remains in recent data. Research to understand the drop-off is in progress; this letter is intended as a caution to users of the data. Our findings underscore the importance of regular ozonesonde data evaluation.

A Post-2013 Drop-off in Total Ozone at a Third of Global Ozonesonde Stations: ECC Instrument Artifacts?

Ryan M. Stauffer[1,2], Anne M. Thompson[2], Debra E. Kollonige[3,2], Jacquelyn C. Witte[2*] David W. Tarasick[4], Jonathan Davies[4], Holger Vömel[5], Gary A. Morris[6], Roeland Van Malderen[7], Bryan J. Johnson[8], Richard R. Querel[9], Henry B. Selkirk[10,2], Rene Stübi[11], and Herman G. J. Smit[12]

[1]Earth System Science Interdisciplinary Center, University of Maryland, College Park, MD, USA

[2]Atmospheric Chemistry and Dynamics Lab, NASA/GSFC, Greenbelt, MD, USA

*Now at National Center for Atmospheric Research Earth Observations Laboratory, Boulder, CO, USA

[3]Science Systems and Applications, Inc., Lanham, MD, USA

[4]Environment and Climate Change Canada, Downsview, ON, CA

[5]National Center for Atmospheric Research Earth Observations Laboratory, Boulder, CO, USA

[6]St. Edwards University, Austin, TX, USA

[7]Royal Meteorological Institute of Belgium, Uccle (Brussels), Belgium

[8]Global Monitoring Laboratory, NOAA Earth System Research Laboratory, Boulder, CO, USA

[9]National Institute of Water & Atmospheric Research (NIWA), Lauder, NZ

[10]Universities Space Research Association, Columbia, MD, USA

[11]Federal Office of Meteorology and Climatology, MeteoSwiss, Aerological Station, Payerne, Switzerland

[12]Institute of Chemistry and Dynamics of the Geosphere: Troposphere, Jülich Research Centre, Jülich, Germany

Corresponding author: Ryan M. Stauffer (ryan.m.stauffer@nasa.gov)

Key Points:

- We report a drop in ozonesonde total column O_3 of 3-7 % relative to independent measurements at a third of sites beginning around 2014
- Comparisons with satellite stratospheric O_3 profiles show the artifact loss peaking at 5-10 % or more in the middle and upper stratosphere

- Changes in the ozonesonde instrument are apparently associated with the drop-off, but no single factor appears to be the cause

Keywords: ECC Ozonesonde, Aura, OMI, MLS, Suomi-NPP, OMPS

Index Terms: 0394, 0365, 9815

Abstract

An international effort to improve ozonesonde data quality and to reevaluate historical records has made significant improvements in the accuracy of global network data. However, between 2014 and 2016, ozonesonde total column ozone (TCO; O_3) at 14 of 37 regularly reporting stations exhibited a sudden drop-off relative to satellite measurements. The ozonesonde TCO drop is 3-7 % compared to satellite and ground-based TCO, and 5-10 % or more compared to satellite stratospheric O_3 profiles, compromising the use of recent data for trends, although they remain reliable for other uses. Hardware changes in the ozonesonde instrument are likely a major factor in the O_3 drop-off, but no single property of the ozonesonde explains the findings. The bias remains in recent data. Research to understand the drop-off is in progress; this letter is intended as a caution to users of the data. Our findings underscore the importance of regular ozonesonde data evaluation**.**

Plain Language Summary

Balloon-borne ozonesondes provide accurate measurements of atmospheric ozone (O_3) from the surface to above 30 km with high vertical resolution. Dozens of global stations have regularly launched ozonesondes for decades, and they provide vital information for improving O_3-measuring satellite algorithms, tracking recovery of the stratospheric O_3 layer, and our understanding of surface to lower stratospheric O_3 changes in an evolving climate. We present the discovery of an apparent instrument artifact that has caused total column O_3 measurements from about a third of global stations to drop by 3-7 % starting in 2014-2016, limiting their suitability for calculating O_3 trends. Work is underway to solve the problem, but the exact cause of the drop is still unknown. This letter serves as a caution to the community of ozonesonde data users.

1 Background: The Ozonesonde Instrument and Data Quality Assurance

The electrochemical concentration cell (ECC) ozonesonde measures ozone (O_3) profiles from the surface through the mid-stratosphere (~5 hPa). Ozone is measured via a chemical reaction from bubbling ambient O_3 into a two-chamber electrochemical cell containing a potassium iodide (KI) solution (sensing solution type or SST, which refers to the solution KI and pH buffer concentration; see Table 1). The ECC is launched on a weather balloon coupled to a radiosonde that transmits O_3 partial pressure simultaneously with pressure, temperature, humidity (PTU), and GPS-derived wind data to a ground station approximately once a second. With a 20-30 s response time, the effective vertical resolution of the O_3 signal is ~150 m.

Because each ozonesonde is a new instrument that must be prepared before launch, it is essential to standardize instrument preparation, operations, and the treatment of raw data. In the past decade, a panel of researchers have engaged in both individual and collective tests of instrumentation, meeting regularly to discuss quality assurance and to develop standard operating procedures (SOP) in an activity designated Assessment of SOP for Ozonesondes (ASOPOS). Current SOP were published in **Smit and ASOPOS (2014**). The main sources of instrument variability are the instrument type (there are two major manufacturers of ECC instruments, which we call “Type1” and “Type2”), the composition of the SST, conditioning protocol, and post-processing; these parameters are given in the metadata for each record.

ASOPOS has also published guidelines for reprocessing sonde data records that may be affected by deliberate or inadvertent ECC preparation changes. For example, the ASOPOS recommendation is to deploy each ECC type with a different SST, even though the two types operate on the exact same measurement principle. If a station changes only one of these variables, the resulting step change in O_3 is considered an instrumental artifact. Reprocessing is carried out to compensate for such changes, and the data are said to be homogenized (**Smit and ASOPOS, 2012**; **Deshler et al., 2017**). Both the SOP and reprocessing guidelines are based on laboratory (**Smit et al., 2007**) and field tests (**Deshler et al., 2008**) in which different sensors are compared with a standard O_3 reference photometer. In the lab, tests are made with 2-4 ECC sensors operating in a closed chamber that simulates a standard profile over a 2-hr "flight." Field tests compare instruments on a single gondola launched with a balloon capable of lifting the payload to ~30 km.

During the period 2013 through 2017, data from more than 25 ozonesonde stations were reprocessed (**Tarasick et al., 2016; Van Malderen et al., 2016; Thompson et al., 2017; Witte et al., 2017; Sterling et al., 2018; Witte et al., 2019**). In general, the reprocessed data show significant improvements in comparisons with independent total column ozone (TCO) measurements. Reprocessed data at 12 of 14 SHADOZ stations agree to within 2 % of satellite and ground-based TCO measurements (**Thompson et al., 2017**), compared to offsets > 8 % at half of the stations for the period prior to 2005 in **Thompson et al. (2007)**. Improvements in tropical mid-stratospheric O_3 values also led to better agreement with the Aura Microwave Limb Sounder (MLS) profiles (2005-2017; **Witte et al., 2017**).

In spite of the reprocessing successes, the homogenized data for two tropical stations (Costa Rica and Hilo) displayed sharp 5 % drop-offs in TCO relative to satellite measurements after 2014; at Hilo a simultaneous discrepancy appeared relative to the Mauna Loa Dobson spectrometer (**Thompson et al., 2017; Sterling et al., 2018**). The drop-off was also observed in the original datasets, ruling out the reprocessing as the cause. In contrast, NOAA's Boulder, CO, site, which used the same instrumentation and SST, did not appear to be similarly affected.

Hypothesized causes for these findings, e.g., hardware changes in the 2011-2016 period (the company manufacturing Type1 ECCs changed ownership twice) or the non-standard SST supplied by NOAA to the above-mentioned sites, were tested along with other variables in a new series of chamber tests (JOSIE; Jülich Ozonesonde Intercomparison Experiments) in late 2017. Initial results from the 80 chamber profiles in JOSIE-SHADOZ could not explain the drop-off behavior (**Thompson et al., 2019**), and the cause remained unsolved.

Because ozonesonde profiles are relied upon as the foundation for satellite O_3 retrievals and validation, we re-examine the agreement among sonde, satellite, and ground-based TCO with two more years of data from the SHADOZ and NOAA networks to determine if the drop-offs reported in **Thompson et al. (2017)** and **Sterling et al. (2018)** persist. We also extend these analyses to the global network during the Aura satellite era of October 2004 to present. We find that over a third of these 37 stations exhibit an instrumental artifact drop-off in TCO after 2013, caused by a decline in stratospheric O_3 measured by the ECC instruments. Instrumental factors are investigated but no definitive explanation for these findings has yet emerged. In **Section 2** data sources and statistical methods are described. **Section 3** describes results and potential changes to the ECC instrument and factors that require further investigation. **Section 4** is a summary and recommendations for use of data affected by the ECC O_3 drop-off.

2 Data and Methods

2.1 ECC Ozonesonde Data

We selected a total of 37 global ECC ozonesonde sites based on the availability of consistent and up-to-date records during the Aura period from October 2004 to present (i.e. data available within the last few years; an exception is Watukosek which ended in October 2013) to analyze the recent drop in ECC TCO measurements. Currently, 28 of the sites launch Type1 ECCs, and nine launch Type2. Some sites have previously changed ECC types, SST, or both, so the most recent metadata are listed in **Table 1**. The primary evaluation of ozonesonde data is with TCO and stratospheric O_3 measurements from NASA's Aura satellite; sample numbers listed in **Table 1** are from the Aura period only. The ozonesonde data are not normalized to a TCO measurement or an outside data source. We calculate ECC TCO amounts by integrating the ozonesonde O_3 up to 10 hPa or balloon burst, whichever is greater in pressure, and add the **McPeters and Labow (2012)** climatological residual O_3 to that amount. We do not calculate the TCO amount for ozonesondes that fail to reach 30 hPa.

2.2 Satellite and Ground-Based Data

Satellite TCO measurements are from the Aura Ozone Monitoring Instrument (OMI v8.5; **McPeters et al., 2008; McPeters et al., 2015**) and the Suomi-NPP Ozone Mapping Profiler Suite (OMPS v2; **McPeters et al., 2019**). To identify "coincident" satellite overpasses, we limit Level 2 TCO data to within 8 hours and 100 km of the ozonesonde measurement. Sensitivity tests on our screening of coincident satellite TCO data by limiting comparisons based on cloud fraction or a smaller overpass distance to the ECC site had negligible effects on the statistics (less than 1 % change in overall OMI/ECC TCO agreement). Stratospheric O_3 profile measurements are from Aura MLS (**Froidevaux et al., 2008**). We use MLS v4.2 Level 2 O_3 data averaged within one day and 5° latitude and 8° longitude of the ozonesonde launch. MLS data are screened according to the v4.2 Level 2 MLS Data Quality document (**Livesey et al., 2018**).

The OMI and OMPS TCO measurements compare well with the series of Solar Backscatter Ultraviolet instruments and are suitable for TCO trend analysis (**McPeters et al., 2015; 2019**). Aura MLS O_3 measurements in the stratosphere exhibit little drift – the v3.3 measurements are stable to within 1.5 % per decade (**Hubert et al. 2016**; it is presumed the v4.2 data used here have similar stability). Thus, these three satellite instruments are suitable to detect significant changes in the ECC ozonesonde network. Our primary ECC comparisons are with OMI and MLS because of their > 15 year record. OMPS reinforces the OMI and MLS results.

Twenty-three of the 37 ECC sites have a co-located ground-based TCO instrument (**Table 1**). Most sites have a Brewer or Dobson spectrophotometer (or both at Hilo and Tateno); Réunion uses a SAOZ UV-visible spectrometer. ECC TCO comparisons with all three ground-based instrument types are found in **Thompson et al. (2017)**.

2.3 Defining the ECC O_3 Drop-off: Example Sites

To characterize the O_3 drop-off, we separate the sites with unambiguous drops in TCO, which we call "affected" sites, from those called "reference" sites. Affected sites are defined as follows: At each site, the average difference between ECC and OMI TCO for 2004-2013 (nearly a decade of measurements) is computed. A moving, 100-sample average of differences between ECC and OMI TCO for the entire record is compared to the 2004-2013 value. If the moving average falls more than 3 % below the 2004-2013 value, the site is identified as having a drop-off at that date. The identified drop-off dates may occur a few months after a visual "breakpoint" in the time series of ECC and OMI comparisons, but the 100-sample moving average ensures that any drop-off in ECC TCO is sustained over many ozonesonde profiles and is not a temporary feature. The date of drop-off and maximum TCO drop relative to OMI are listed for affected sites in Table 1. For example, **Figure 1a** displays a sudden drop-off relative to OMI at Kelowna in November 2014. The ECC TCO averaged 4.1 % higher than OMI from 2004-2013. The 100-sample moving average fell to +1 % in November 2014, and fell as low as -0.7 % in November 2016 for a maximum 4.7 % drop (Table 1).

The drop-off is identified at Hilo in March 2015 and at Costa Rica in December 2015 (**Figure 1b, c**). Hilo and Costa Rica exhibit maximum drop-offs of 4.0 and 6.2 % relative to OMI. The percent differences between ozonesonde and MLS stratospheric O_3 in the top panels of **Figure 1** show that the drop in ECC O_3 relative to MLS is coincident with the TCO drop.

3 Results and Discussion

3.1 Sites Affected by the ECC O_3 Drop-off

Using the criterion of a > 3 % TCO drop relative to OMI, we find that 14 of 37 sites are affected by a TCO drop-off. **Table 1** lists the affected sites in bold including the maximum TCO drop relative to OMI computed using the 100-sample moving average. A map of all sites examined, with affected sites colored according to the magnitude of TCO drop-off, is shown on **Figure 2**. We define the drop in TCO as relative to OMI because some sites previously exhibited a high bias compared to satellites, with the drop-off actually leading to closer agreement with OMI (e.g. Kelowna in **Figure 1a**).

Dates of the drop in TCO measurements range from January 2014 at San Cristóbal to January 2017 at Edmonton. All but one (Natal) of the affected sites use Type1 ECCs. The magnitude of the TCO drop-off varies considerably. The drop in TCO at Nairobi is a relatively modest 3.2 %, whereas a change of 7.4 % is observed at Yarmouth. It appears that there are two clusters of affected sites, in the tropics and in Canada, with most mid-latitude sites remaining unaffected by a drop-off. In summary, there is inconsistency in TCO drop-off amount, and the drop-off is not a universal problem.

Comparisons similar to **Figure 1** for the remaining 34 sites in **Table 1** are found in the Supplementary Material in **Figures S1a-k and S2a-w**. We note that individual sites show periods of high or low bias compared to OMI and MLS (e.g. Madrid's high bias for a portion of 2009; **Figure S2h**). However, our focus is on sudden drops in O_3 that persist for more than 2 or 3 years in the most recent record, because this appears to be a widespread pattern, affecting much of the global network.

3.2 Comparisons with Aura MLS Stratospheric O_3

Closer comparison of ECC and MLS O_3 profiles in the stratosphere is warranted given the coincidence between the ECC drop-off relative to OMI and OMPS TCO, and apparent ECC drop-off relative to MLS O_3 in **Figure 1**. **Figure 3a** shows a composite of comparisons between MLS and ECC ozonesonde stratospheric O_3 at the 14 affected sites before and after the identified drop-off (dates in **Table 1**). Prior to the drop-off at the 14 affected ECC sites, stratospheric O_3 biases compared to MLS follow the zero line in **Figure 3a** (blue colors). After the drop-off in TCO, the ECC measurements shift 5-10 % lower relative to MLS (red colors), occasionally reaching > 20 % lower than MLS above 10 hPa (the 25th percentile value at the 6.81 hPa MLS level is -20.3 %). **Figure 3b** and **3c** show similar statistics for the reference Type1 and Type2 sites. The comparisons with MLS profiles are split into 2004-2013 and 2014-2019, near the time when many affected sites exhibit the drop-off. **Figure 3b** and **3c** show that there is no comparable drop-off in stratospheric O_3 at the Type1 and Type2 reference sites. **Figure 3a** indicates that the stratospheric O_3 drop-off is the major contributor to the TCO offsets with OMI and OMPS. Time series of ECC comparisons with OMI TCO and MLS partial stratospheric column O_3 in **Figure S3** demonstrate that the drop-off in ECC stratospheric O_3 exactly coincides with the TCO drop. At this point, a similar drop-off in tropospheric O_3 has not been detected and is presumed to be insignificant. Exceptions are two stations, Costa Rica and Hilo, which may be reading low in recent years in the troposphere due to occasional volcanic SO_2 interference (e.g. **Morris et al., 2010**). That is beyond the scope of our study.

3.3 Potential ECC Instrument Factors in the O_3 Drop-off

The ECC O_3 drop-off has been quantified against satellite TCO and satellite O_3 profiles (**Thompson et al., 2017; Sterling et al., 2018**; ground-based comparisons to follow in Section 3.5). Thus, we rule out geophysical factors as the only cause; the drop-off seems to be an instrument artifact, so we consider potential instrumental contributions. Each ECC is built from a number of components that may change over time as the manufacturer or manufacturers' suppliers change. For example, the Type1 instrument changed manufacturer twice between 2011 and 2016. Components that could change and affect the ECC measurements include the chambers holding the sensing solution, the ion bridge between the two cells, the air intake pump, the constant-speed motor, batteries, and the platinum electrodes. A 3-7 % change of response could be caused by loss of O_3 or of molecular iodine to the ECC chamber walls, losses through the internal resistance of the cell, or in-flight changes in the pump and motor efficiency with pressure. The sensing solution composition and the radiosonde model (and interface) are additional considerations (Section 3.6). The ECC serial number is used to evaluate potential instrument/component changes over time.

Figure 4 shows ECC TCO offsets with OMI and OMPS separated by the 13 affected (red on **Figure 4**) and 15 reference (blue on **Figure 4**) Type1 sites. Median, 25th and 75th percentile statistics are shown for every 1000 serial numbers (e.g. 24K = 24000-24999). The affected sites show a low bias for 25K and higher serial numbers, abruptly dropping from a median TCO bias compared to OMI and OMPS of +1.6 % (24K), to -2.6 % (25K). The inconsistency in timing of the ECC drop-off at affected sites is partly due to when the site begins launching serial numbers 25K and above. The reference sites show no such drop, and, in fact, no recent serial number set since 24K has a median bias larger than -1.5 % (30K) for the 12 reference sites. The affected sites show significant negative biases for all serial numbers from 25K to 35K, with a maximum median low bias of -5.4 % for 31K serial numbers. **Figure 4** shows the history of good ECC/satellite agreement at affected Type1 sites throughout the Aura record since October 2004 and prior to the 25K serial numbers, although there are indications of some low-biased measurements from serial numbers 20-22K. The largest deviation for reference Type1 sites is the +1.7 % median bias for 16K serial numbers (**Figure 4**). In summary, before the TCO drop-off at the affected sites, the ECC TCO comparisons with satellite measurements averaged within 1 or 2 %, and comparisons at reference sites remain, on average, within 1 or 2 %.

Figure 4 shows that reference and affected Type1 sites were both launching ECCs with similar serial numbers, so it is puzzling why they show such large discrepancies in their comparisons with satellite TCO after serial number 25K. This commingling of good and poorly-performing Type1 serial numbers, which appear to be distinguishable only by site, tells us that the ECC O_3 drop-off is not due to manufacturing issues for the Type1 ECC alone and that at least one additional secondary factor must play a role in its occurrence.

3.4 Stations with Type2 ECCs

We examined nine Type2 ECC ozonesonde sites for a drop-off and sudden low TCO bias. Statistics of the TCO offset between reference Type2 ECCs and OMI and OMPS are also shown on **Figure 4** in grey. Note that the similar serial numbers between Type1 and Type2 ECCs are a coincidence. The Type2 comparisons show no abrupt downward shift in agreement with satellite TCO as seen at the affected Type1 sites in **Figure 4**. An exception is at Natal (**Figure S1h**).

3.5 ECC Comparisons with Ground-Based TCO Measurements

Of the 37 sites analyzed here, 23 have ground-based TCO measurements to compare against the ECCs (**Table 1**). Example time series of the comparisons between ECCs and the Brewer at Churchill, and the Brewer and Dobson at Hilo are shown in **Figure S4**. The ground-based TCO measurements near Hilo are taken at Mauna Loa (3405 m), which explains why the ECC TCO is higher than the Brewer and Dobson prior to the March 2015 drop-off. Statistics similar to **Figure 4** for the ground-based TCO comparisons are shown in **Figure S5**. The ECC TCO drop-off relative to the ground-based instruments at affected Type1 sites is ~3-4 % after > 25K serial numbers in **Figure S5**. The ground-based comparisons with reference Type1 and Type2 sites are quite variable, and the difference in behavior of affected Type1 ECCs is not as apparent in the ground-based comparisons as it is in the satellite TCO comparisons. This is because several affected sites like Costa Rica, Ascension, Kelowna, and Yarmouth do not have ground-based TCO instruments. Spectrometer data at some affected Canadian sites are also limited by low winter sunlight.

3.6 Possible Sources of the Drop-Off

Around 2010-2012, most of the affected ozonesonde sites examined here switched from the Vaisala RS-80 to RS-92 radiosonde, or from RS-80 to the InterMet iMet radiosonde. The radiosonde pressure measurements affect the ECC O_3 calculation and altitude registration, so a change from non-GPS RS-80 to GPS-enabled RS-92 and iMet radiosondes can lead to pressure measurement changes, which translate to O_3 changes (**Steinbrecht et al., 2008; Stauffer et al., 2014; Inai et al., 2015**). Some sites (e.g. Lauder in 2015) switched radiosondes again from RS-92 to the RS-41. An example of an RS-80 to iMet transition at Hilo is shown in **Figure S6**. There is a shift in mid-stratospheric pressure and temperature measurements with the transition to iMet in 2011-2012, but this change occurs more than two years before the Hilo low O_3 bias in March 2015. Similar mismatches between radiosonde changes and the ECC drop-off are found at other sites. Costa Rica switched from RS-80 to iMet radiosondes in 2012-2013, but the drop-off did not occur until December 2015 (**Thompson et al., 2017**). Nairobi switched from RS-80 to RS-92 radiosondes in 2010, but there was no drop-off until July 2016. We therefore rule out radiosonde changes as the primary cause of the ECC O_3 drop-off.

The drop-off is found at sites that use a variety of SSTs (**Table 1**) and three different radiosonde types (RS-92 or 41 and iMet). Sites that are seemingly unaffected, e.g. Trinidad Head, Boulder, and Huntsville, all use the same 1.0 % KI with 1/10th buffer SST and iMet radiosonde combination as Hilo and Costa Rica (**Figure 1**). We have not fully explored the effects of different SSTs on the O_3 drop-off, but given that all three SSTs currently in use are affected (**Table 1**), it does not appear that SST is the main factor.

The ASOPOS 2.0 panel is performing additional experiments and analyses to identify possible sources of the O_3 drop-off. Tests include examining the different radiosonde interface boards and batteries used on Type1 ECC sondes, reviewing site ECC preparation procedures, and experiments with older Type1 ECCs manufactured before the drop-off began. Possible changes in behavior of the pump, pump motor, or batteries at low stratospheric pressures and temperatures, are obvious candidate factors and have been considered, but preliminary results have not identified significant differences. Both Type1 and Type2 ozonesondes, four different sensing SSTs, and varying preparation procedures were tested in the 2017 JOSIE-SHADOZ experiment (**Thompson et al., 2019**), and a preliminary analysis did not reveal any signs of the drop-off in those data. In-depth analysis of the 80 profiles from JOSIE-SHADOZ should help identify the causes and magnitudes of contributing factors like SST to the ECC O_3 drop-off.

4 Summary and Recommendations for Affected Data

Since 2014-2016, we have observed a drop-off in ECC ozonesonde TCO and stratospheric O_3 at 14 ECC global ozonesonde sites, 13 of which launch Type1 ECC ozonesondes. The TCO drop is 3-7 % compared to OMI TCO measurements, and the stratospheric O_3 drop can be greater than 10 % compared to MLS O_3 profiles in the mid-stratosphere. The low bias is notably absent at half of the 28 Type1 sites that we examined. Except for Natal, there is no significant drop-off or change in bias for Type2 ECC ozonesondes during similar years. Because the drop-off varies greatly from site-to-site, it is likely that it is influenced by station-specific procedures yet to be identified. The ECC O_3 drop-off has more than one single cause (i.e. both instrument- and station-specific influences).

Affected data archives such as SHADOZ (https://tropo.gsfc.nasa.gov/shadoz/), the World Ozone and Ultraviolet Data Centre (WOUDC.org), and the Network for the Detection of Atmospheric Composition Change (NDACC; ndaccdemo.org) are posting caveats and flagging affected profiles. Ongoing research is directed at identifying the cause of the low O_3 bias.

We emphasize that all reprocessed data are expected to be more accurate than unhomogenized data. For affected sites, data before the drop-off are highly reliable and even affected data are accurate for satellite validation and algorithms, process studies, and model evaluation because the apparent drop-off averages less than 5 %. However, the affected data are judged not appropriate for calculations of TCO or stratospheric trends or satellite drift.

Acknowledgments

Funding for this work was provided through support of SHADOZ by the NASA Upper Air Research Program (UARP; Dr. Kenneth Jucks program manager) to NASA/GSFC (A. M. Thompson, PI). SHADOZ v6.0 ozonesonde data were downloaded from the NASA/GSFC archive at https://tropo.gsfc.nasa.gov/shadoz/. Canadian reprocessed ozonesonde data were provided by co-author D. Tarasick, and reprocessed Uccle ozonesonde data were provided by co-author R. Van Malderen. NOAA ozonesonde data (Boulder, Huntsville, and Trinidad Head) were downloaded at ftp://aftp.cmdl.noaa.gov/data/ozwv/Ozonesonde/. All other ozonesonde data and all ground-based TCO data are available at the World Ozone and Ultraviolet Data Centre (WOUDC; https://woudc.org/data/explore.php?lang=en). Aura MLS v4.2 Level 2 O_3 overpass data were downloaded at https://avdc.gsfc.nasa.gov/pub/data/satellite/Aura/MLS/V04/L2GPOVP/O3/. OMI and OMPS Level 2 TCO overpass data were downloaded at https://avdc.gsfc.nasa.gov/pub/data/satellite/Aura/OMI/V03/L2OVP/OMTO3/ and https://avdc.gsfc.nasa.gov/pub/data/satellite/Suomi_NPP/L2OVP/NMTO3-L2/.

References

Deshler, T., et al. (2008), Atmospheric comparison of electrochemical cell ozonesondes from different manufacturers, and with different cathode solution strengths: The Balloon Experiment on Standards for Ozonesondes, *J. Geophys. Res*., 113, D04307, doi:10.1029/2007JD008975.

Deshler, T., R. Stuebi, F. J. Schmidlin, J. L. Mercer, H. G. J. Smit, B. J. Johnson, R. Kivi, R., and B. Nardi (2017), Methods to homogenize electrochemical concentration cell (ECC) ozonesonde measurements across changes in sensing solution concentration or ozonesonde manufacturer, *Atmos. Meas. Tech*., 10, 2021–2043, doi:10.5194/amt-10-2021-2017.

Froidevaux, L., et al. (2008), Validation of Aura Microwave Limb Sounder stratospheric ozone measurements, *J. Geophys. Res*., 113, D15S20, doi:10.1029/2007JD008771.

Hubert, D., et al. (2016), Ground-based assessment of the bias and long-term stability of 14 limb and occultation ozone profile data records, *Atmos. Meas. Tech*., 9, 2497–2534, https://doi.org/10.5194/amt-9-2497-2016.

Inai, Y., M. Shiotani, M. Fujiwara, F. Hasebe, and H. Vömel (2015), Altitude misestimation caused by the Vaisala RS80 pressure bias and its impact on meteorological profiles, *Atmos. Meas. Tech.,* 8, 4043–4054, https://doi.org/10.5194/amt-8-4043-2015.

Livesey, N. J., et al. (2018), Version 4.2x-3.1 Level 2 data quality and description document, JPL D-33509 Rev. B. [Available at https://mls.jpl.nasa.gov/data/v4-2_data_quality_document.pdf.]

McPeters, R., Kroon, M., Labow, G., Brinksma, E., Balis, D., Petropavlovskikh, I., Veefkind, J. P., Bhartia, P. K., and Levelt, P. F. (2008), Validation of the Aura Ozone Monitoring

Instrument total column ozone product, *J. Geophys. Res*., 113, D15S14, doi:10.1029/2007JD008802.

McPeters, R. D., and G. J. Labow (2012), Climatology 2011: An MLS and sonde derived ozone climatology for satellite retrieval algorithms, *J. Geophys. Res*., 117, D10303, doi:10.1029/2011JD017006.McPeters, R. D., Frith, S., and Labow, G. J. (2015), OMI total column ozone: extending the long-term data record, *Atmos. Meas. Tech*., 8, 4845–4850, https://doi.org/10.5194/amt-8-4845-2015.

McPeters, R., Frith, S., Kramarova, N., Ziemke, J., and Labow, G. (2019), Trend quality ozone from NPP OMPS: the version 2 processing, *Atmos. Meas. Tech*., 12, 977–985, https://doi.org/10.5194/amt-12-977-2019.

Morris, G. A., W. D. Komhyr, J. Hirokawa, J. Flynn, B. Lefer, N. Krotkov, F. Ngan (2010), A balloon sounding technique for measuring SO_2 plumes, *J. Atmos. Oceanic Technol.*, 27, 1318–1330. doi: 10.1175/2010JTECHA1436.1

Smit, H. G. J., et al. (2007), Assessment of the performance of ECC-ozonesondes under quasi-flight conditions in the environmental simulation chamber: Insights from the Jülich Ozone Sonde Intercomparison Experiment (JOSIE), *J. Geophys. Res*., 112, D19306, doi:10.1029/2006JD007308.

Smit, H. G. J., and the Panel for the Assessment of Standard Operating Procedures for Ozonesondes (ASOPOS) (2012), Guidelines for homogenization of ozonesonde data, SI2N/O3S-DQA activity as part of “Past changes in the vertical distribution of ozone assessment”. [Available at http://www-das.uwyo.edu/%7Edeshler/NDACC_O3Sondes/O3s_DQA/O3S-DQA-Guidelines%20Homogenization-V2-19November2012.pdf.]

Smit, H. G. J., and the Panel for the Assessment of Standard Operating Procedures for Ozonesondes (ASOPOS) (2014), Quality assurance and quality control for ozonesonde measurements in GAW, World Meteorological Organization, GAW Report 201. [Available at http://www.wmo.int/pages/prog/arep/gaw/documents/FINAL_GAW_201_Oct_2014.pdf.]

Stauffer, R. M., G. A. Morris, A. M. Thompson, E. Joseph, G. J. R. Coetzee, and N. R. Nalli (2014), Propagation of radiosonde pressure sensor errors to ozonesonde measurements, *Atmos. Meas. Tech.*, 7, 65–79, doi:10.5194/amt-7-65-2014.

Steinbrecht, W., H. Claude, F. Schönenborn, U. Leiterer, H. Dier, H., and E. Lanzinger (2008), Pressure and temperature differences between Vaisala RS80 and RS92 radiosonde systems, *J. Atmos. Ocean. Tech.*, 25, 909-927, doi:10.1175/2007JTECHA999.1.

Sterling, C. W., Johnson, B. J., Oltmans, S. J., Smit, H. G. J., Jordan, A. F., Cullis, P. D., et al. (2017). Homogenizing and estimating the uncertainty in NOAA's long term vertical ozone profile records measured with the electrochemical concentration cell ozonesonde. *Atmos. Meas. Tech*., 11, 3661-3687, https://doi.org/10.5194/amt-2017-397

Tarasick, D. W., J. Davies, H. G. J. Smit, and S. J. Oltmans (2016), A re-evaluated Canadian ozonesonde record: Measurements of the vertical distribution of ozone over Canada from 1966 to 2013, *Atmos. Meas. Tech.*, 9, 195–214, doi:10.5194/amt-9-195-2016.

Thompson, A. M., J. C. Witte, H. G. J. Smit, S. J. Oltmans, B. J. Johnson, V. W. J. H. Kirchhoff, and F. J. Schmidlin (2007), Southern Hemisphere Additional Ozonesondes (SHADOZ) 1998–2004 tropical ozone climatology: 3. Instrumentation, station-to-station variability, and evaluation with simulated flight profiles, *J. Geophys. Res*., 112, D03304, doi:10.1029/2005JD007042.

Thompson, A. M., Witte, J. C., Sterling, C., Jordan, A., Johnson, B. J., Oltmans, S. J., et al. (2017). First reprocessing of Southern Hemisphere Additional Ozonesondes (SHADOZ) profiles (1998-2016). 2. Comparisons with satellites and ground-based instruments, *J. Geophys. Res. Atmos.*, 122, 13000-13025, https://doi.org/10.1002/2017JD27406

Thompson, A. M., H. G. J. Smit, J. C. Witte, R. M. Stauffer, B. J. Johnson, G. Morris, et al. (2019), Ozonesonde quality assurance: The JOSIE-SHADOZ (2017) Experience, *Bull. Amer. Met. Soc.*, 100 (1), 155-171, https://doi.org/10.1175/BAMS-D-17-0311.1

Van Malderen, R., Allaart, M. A. F., De Backer, H., Smit, H. G. J., and De Muer, D. (2016). On instrumental errors and related correction strategies of ozonesondes: Possible effect on calculated ozone trends for the nearby sites Uccle and De Bilt. *Atmos. Meas.Tech.*, 9, 3793–3816. https://doi.org/10.5194/amt-9-3793-2016.

Witte, J. C., Thompson, A. M., Smit, H. G. J., Fujiwara, M., Posny, F., Coetzee, G. J. R., et al. (2017). First reprocessing of Southern Hemisphere ADditional Ozone-sondes (SHADOZ) profile records (1998–2015): 1. Methodology and evaluation. *J. Geophys. Res. Atmos*, 122, 6611–6636. https://doi.org/10.1002/2016JD026403.

Witte, J. C., Thompson, A. M., Schmidlin, F. J., Northam, E. T., Wolff, K. R., and Brothers, G. B. (2019). The NASA Wallops Flight Facility digital ozonesonde record: Reprocessing, uncertainties, and dual launches. Journal of Geophysical Research: Atmospheres, 124, 3565–3582. https://doi.org/10.1029/2018JD030098

WMO/GAW Ozone Monitoring Community: World Meteorological Organization-Global Atmosphere Watch Program (WMO-GAW)/World Ozone and Ultraviolet Radiation Data Centre (WOUDC) [Data] (2015), available at: https://woudc.org (last access: 25 September 2019), https://doi.org/10.14287/10000008

Table 1. ECC type, total number of samples, latitude, longitude, Solution type (SST) (KI concentration, buffer strength), the 25th percentile, mean, and 75th percentile TCO differences with OMI (October 2004-present), date of drop-off and maximum amount of drop-off in the 100-sample moving mean (see Figure 1) if applicable, and ground-based instrument if applicable are listed. Sites with a > 3 % drop in TCO relative to OMI (Section 2.3) are in bold. Type1 is EnSci (Westminster, CO, USA) and Type2 is Science Pump Corporation (SPC; Camden, NJ, USA). Note that Japanese stations Sapporo, Tateno, and Naha launched carbon-iodine ozonesondes prior to 2008-2009, and those are not considered here.

Site	ECC	N	Lat (°)	Lon (°)	KI SST	OMI 25th (%)	OMI μ (%)	OMI 75th (%)	Drop-Off	TCO Drop (%)	Ground TCO
Alert	**Type1**	**645**	**82.49**	**-62.34**	**1.0%, Full**	**-0.6**	**1.0**	**3.1**	**02/2016**	**-4.3**	**Brewer**
Eureka	**Type1**	**922**	**79.98**	**-85.94**	**1.0%, Full**	**-0.4**	**1.9**	**4.5**	**04/2016**	**-4.2**	**Brewer**
Resolute	Type1	540	74.7	-94.96	1.0%, Full	-4.8	-2.2	0.6	N/A	N/A	Brewer
Churchill	**Type1**	**417**	**58.74**	**-94.07**	**1.0%, Full**	**-1.1**	**0.7**	**3.3**	**11/2016**	**-5.5**	**Brewer**
Edmonton	**Type1**	**674**	**53.54**	**-114.1**	**1.0%, Full**	**-2.9**	**-0.4**	**2.9**	**01/2017**	**-3.9**	**Brewer**
Goose Bay	Type1	663	53.31	-60.36	1.0%, Full	-1.9	0.7	3.4	N/A	N/A	Brewer
De Bilt	Type2	736	52.1	5.18	1.0%, Full	-0.6	1.3	2.9	N/A	N/A	Brewer
Uccle	Type1	2140	50.8	4.35	0.5%, Half	-1.5	0.0	2.0	N/A*	N/A	Brewer
Kelowna	**Type1**	**664**	**49.93**	**-119.4**	**1.0%, Full**	**1.4**	**3.4**	**5.9**	**11/2014**	**-4.7**	**N/A**
Payerne	Type1	2191	46.49	6.57	0.5%, Half	-2.5	-0.7	0.9	N/A*	N/A	N/A
Yarmouth	**Type1**	**616**	**43.87**	**-66.11**	**1.0%, Full**	**-0.2**	**2.4**	**5.3**	**02/2015**	**-7.4**	**N/A**
Sapporo	Type1	373	43.06	141.33	0.5%, Half	1.0	2.7	4.4	N/A	N/A	Dobson
Trinidad Head	Type1	772	40.8	-124.16	1.0%, 1/10	-2.1	-0.2	1.6	N/A	N/A	N/A
Madrid	Type2	680	40.47	-3.58	1.0%, Full	-2.1	-0.3	1.6	N/A	N/A	Brewer
Boulder	Type1	816	40	-105.25	1.0%, 1/10	-2.1	-0.3	2.0	N/A	N/A	Dobson
Wallops Island	Type2	773	37.93	-75.48	1.0%, Full	-2.5	-0.3	1.8	N/A	N/A	Dobson
Tateno	Type1	430	36.06	140.13	0.5%, Half	0.8	2.6	4.3	N/A	N/A	Dobson, Brewer
Huntsville	Type1	759	34.72	-86.64	1.0%, 1/10	-1.6	0.0	1.9	N/A	N/A	N/A
Naha	Type1	403	26.21	127.69	0.5%, Half	0.2	1.7	3.5	N/A	N/A	Dobson
Hong Kong	Type2	690	22.31	114.17	1.0%, Full	-7.0	-4.6	-2.1	N/A	N/A	N/A
Hanoi	Type1	264	21.01	105.8	0.5%, Half	-4.1	-1.8	0.5	N/A	N/A	N/A
Hilo	**Type1**	**711**	**19.43**	**-155.04**	**1.0%, 1/10**	**-3.7**	**-1.9**	**0.2**	**03/2015**	**-4.0**	**Dobson, Brewer**
Costa Rica	**Type1**	**605**	**9.94**	**-84.04**	**1.0%, 1/10**	**-3.1**	**-0.8**	**1.9**	**12/2015**	**-6.2**	**N/A**
Paramaribo	Type2	517	5.8	-55.21	1.0%, Full	-5.0	-2.5	-0.1	N/A	N/A	Brewer
Kuala Lumpur	Type1	264	2.73	101.27	0.5%, Half	-7.3	-4.5	-1.3	N/A	N/A	N/A
San Cristobal	**Type1**	**168**	**-0.92**	**-89.62**	**1.0%, 1/10**	**-4.9**	**-0.8**	**2.4**	**01/2014**	**-4.7**	**N/A**
Nairobi	**Type1**	**596**	**-1.27**	**36.8**	**0.5%, Half**	**-3.7**	**-2.1**	**-0.4**	**07/2016**	**-3.2**	**N/A**
Natal	**Type2**	**400**	**-5.42**	**-35.38**	**1.0%, Full**	**-3.6**	**-1.5**	**1.0**	**04/2016**	**-3.5**	**Dobson**
Watukosek	Type1	115	-7.5	112.6	2.0%, None	-3.4	-1.9	0.4	end 10/2013	N/A	N/A
Ascension	**Type1**	**394**	**-7.58**	**-14.24**	**0.5%, Half**	**-6.0**	**-2.8**	**0.4**	**03/2016**	**-4.2**	**N/A**
Samoa	**Type1**	**474**	**-14.23**	**-170.56**	**1.0%, 1/10**	**-3.0**	**-1.2**	**0.9**	**07/2016**	**-3.9**	**Dobson**
Fiji	**Type1**	**200**	**-18.13**	**178.4**	**1.0%, 1/10**	**-3.1**	**-0.5**	**2.2**	**05/2015**	**-4.8**	**N/A**
Réunion	Type1	449	-21.06	55.48	0.5%, Half	-2.0	0.3	2.4	N/A	N/A	SAOZ
Irene	Type2	212	-25.9	28.22	1.0%, Full	-1.3	1.3	4.3	N/A	N/A	Dobson

Broadmeadows	Type2	667	-37.69	144.95	1.0%, Full	-0.9	0.6	2.7	N/A	N/A	Dobson
Lauder	Type1	705	-45	169.68	0.5%, Half	-3.3	-1.3	0.8	N/A	N/A	Dobson
Macquarie	Type2	675	-54.5	158.95	1.0%, Full	-4.6	-2.4	0.1	N/A	N/A	Dobson

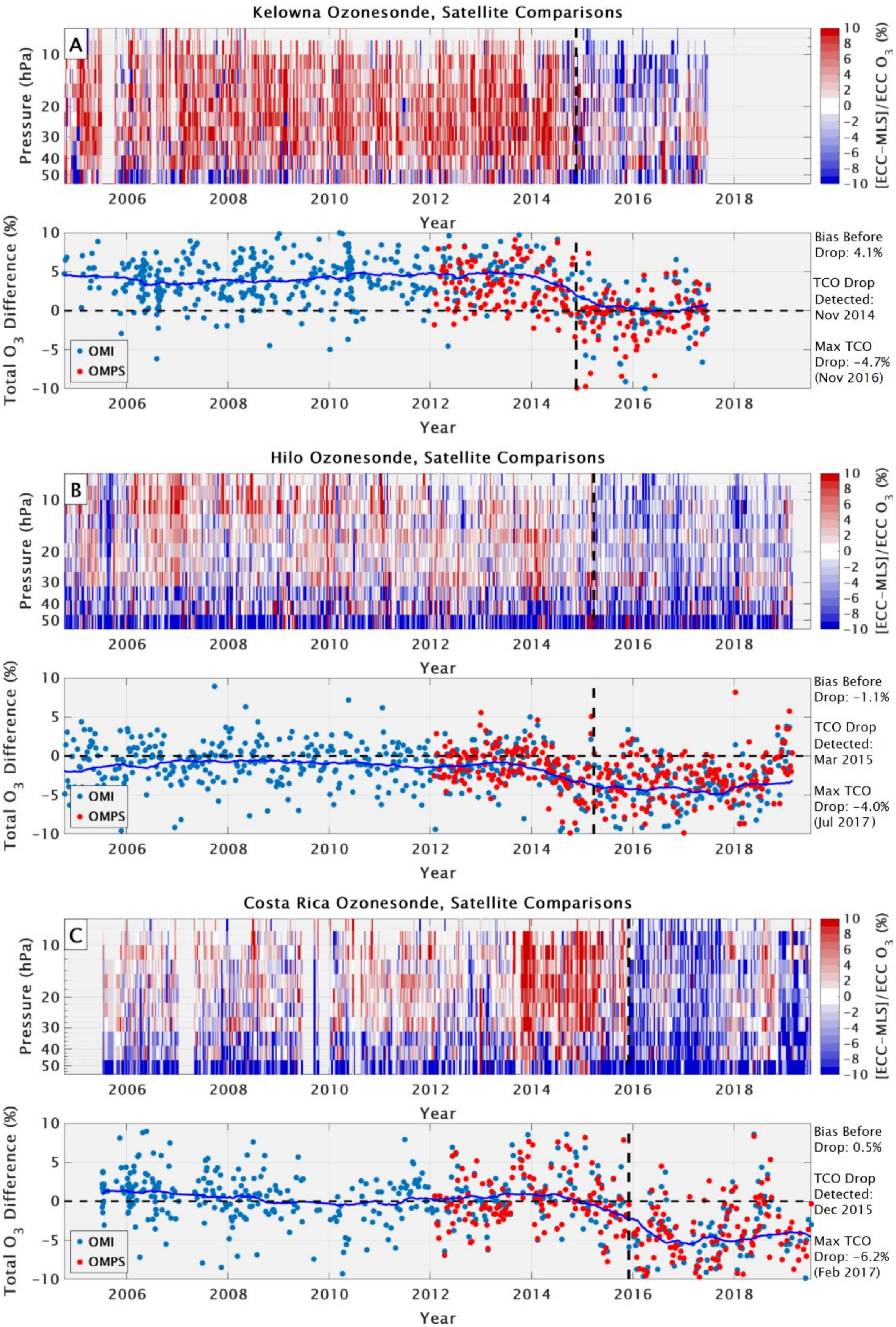

Kelowna Ozonesonde, Satellite Comparisons
A
Pressure (hPa)
[ECC–MLS]/ECC O3 (%)
Year
Total O3 Difference (%)
OMI
OMPS
Bias Before Drop: 4.1%
TCO Drop Detected: Nov 2014
Max TCO Drop: −4.7% (Nov 2016)
Hilo Ozonesonde, Satellite Comparisons
B
Bias Before Drop: −1.1%
TCO Drop Detected: Mar 2015
Max TCO Drop: −4.0% (Jul 2017)
Costa Rica Ozonesonde, Satellite Comparisons
C
Bias Before Drop: 0.5%
TCO Drop Detected: Dec 2015
Max TCO Drop: −6.2% (Feb 2017)

467

Figure 1. Time series of comparisons at Kelowna (A; data end in June 2017), Hilo (B), and Costa Rica (C) between ECC ozonesondes and Aura MLS stratospheric O_3 profiles (top panels), and OMI (blue dots) and OMPS (red dots) TCO (bottom panels). Red or blue colors on the top panels indicate where the ECC O_3 is greater or less than MLS. Horizontal dashed lines indicate the 0 % line for TCO comparisons. Vertical dashed lines indicate the date of the drop-off at each site (see Table 1 for dates), marked by a TCO drop of 3 % relative to the 2004-2013 average difference in OMI and ECC TCO comparisons (blue line on bottom panels).

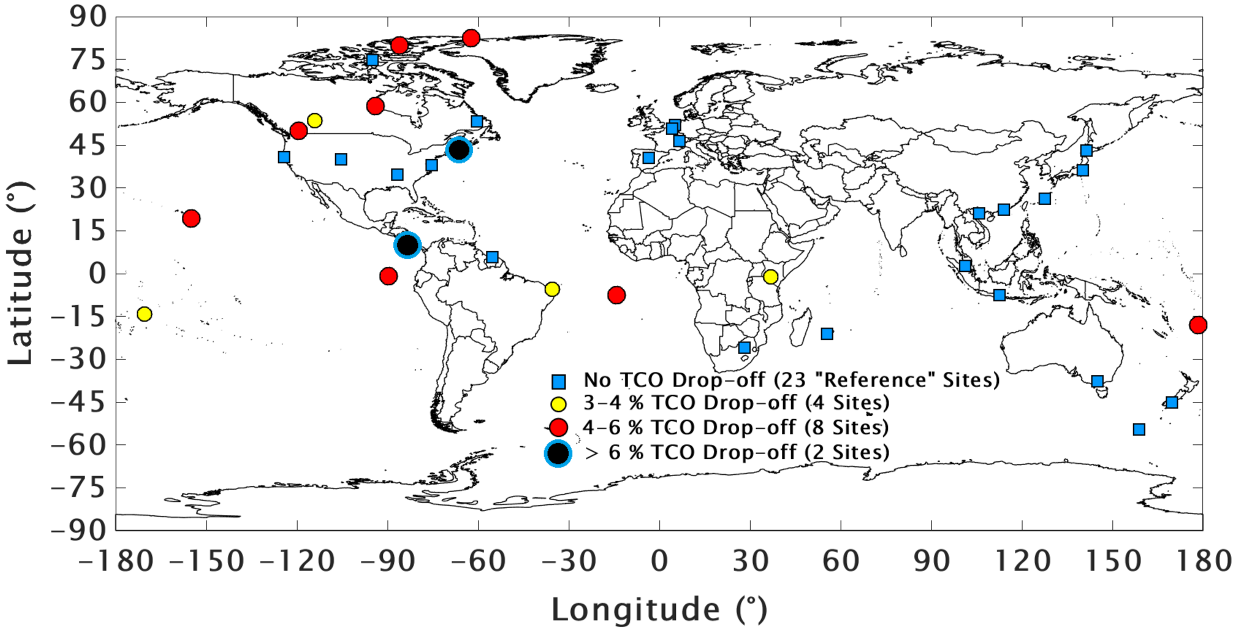

Figure 2. Map of all 37 ECC ozonesonde sites considered in this study. The blue squares indicate sites that show no detectable TCO drop-off relative to OMI. We call these sites "reference" sites. The yellow, red, and black dots indicate sites that exhibit maximum drops of 3-4 %, 4-6 %, and over 6 % (Table 1) relative to OMI TCO. The method for computing the values shown on this figure and in Table 1 are explained in Section 2.3.

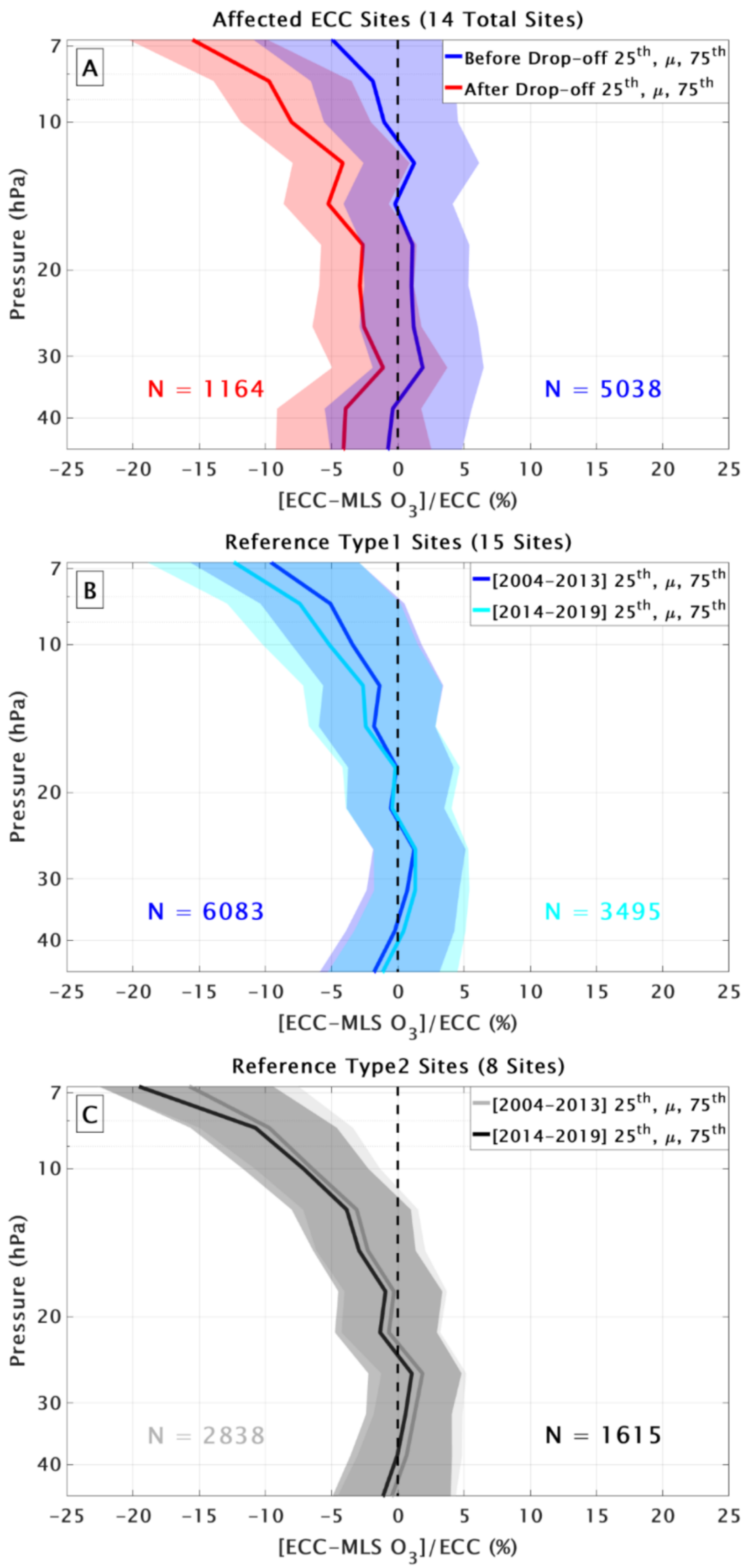
Affected ECC Sites (14 Total Sites)
A
Before Drop-off 25th, μ, 75th
After Drop-off 25th, μ, 75th
N = 1164
N = 5038
Pressure (hPa)
[ECC−MLS O3]/ECC (%)
Reference Type1 Sites (15 Sites)
B
[2004-2013] 25th, μ, 75th
[2014-2019] 25th, μ, 75th
N = 6083
N = 3495
Pressure (hPa)
[ECC−MLS O3]/ECC (%)
Reference Type2 Sites (8 Sites)
C
[2004-2013] 25th, μ, 75th
[2014-2019] 25th, μ, 75th
N = 2838
N = 1615
Pressure (hPa)
[ECC−MLS O3]/ECC (%)

Figure 3. A composite of comparisons between ECC ozonesonde and Aura MLS stratospheric O_3 profiles from before the drop-off at each site (A; blue; dates of drop-off are in Table 1), and during the period after the drop-off (red). Reference Type1 (B) and Type2 (C) sites were split into 2004-2013 and 2014-2019 comparisons to show that there has been no comparable drop-off in stratospheric O_3 around the same period. The shading indicates the 25th to 75th percentile, with mean values shown by the solid lines. ECC sonde sample numbers are shown for each period in the lower portion of the figure.

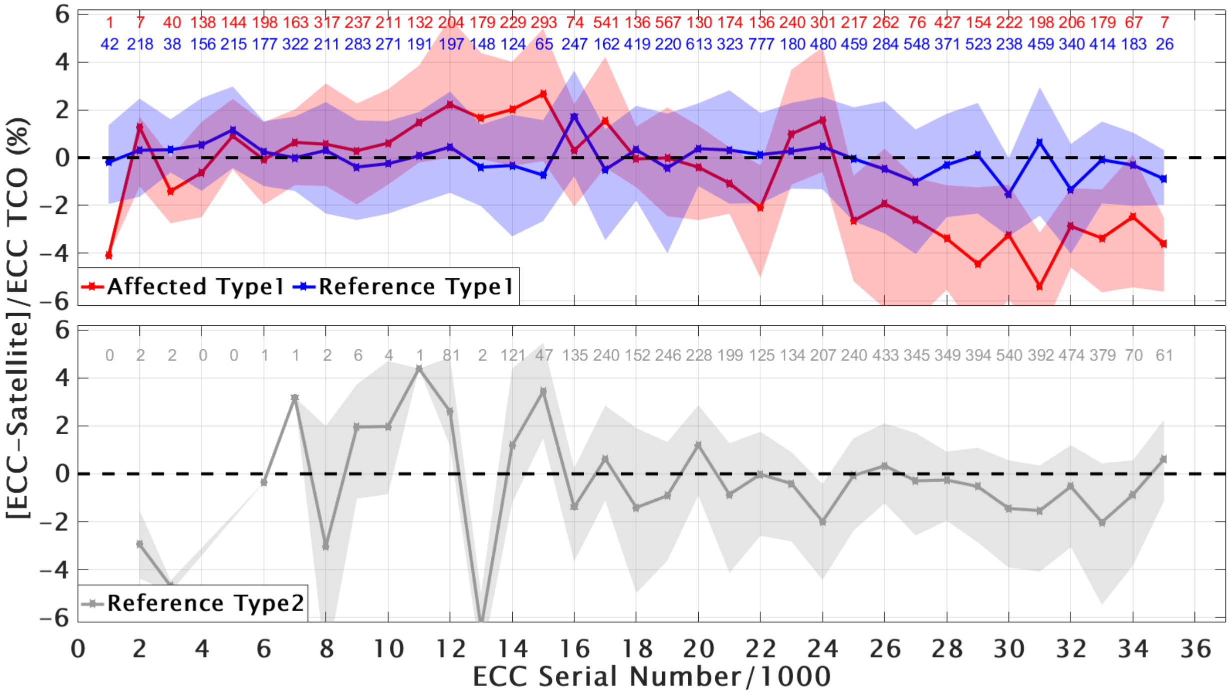

Figure 4. Median (lines) and 25th to 75th (shading) percentiles of comparisons between ECC and OMI and OMPS TCO. The comparisons are separated by every 1000 serial numbers for Type1 (top) and Type2 (bottom) ECCs. The Type1 ECCs are separated into affected (red) and reference (blue) stations. Natal, the only affected Type2 site, is not included in this figure. The number of samples for each serial number bin are shown at the top of each panel.

Geophysical Research Letters

Supporting Information for

A Post-2013 Drop-off in Total Ozone at a Third of Global Ozonesonde Stations: ECC Instrument Artifacts?

Ryan M. Stauffer[1,2], Anne M. Thompson[2], Debra E. Kollonige[3,2], Jacquelyn C. Witte[2*], David W. Tarasick[4], Jonathan Davies[4], Holger Vömel[5], Gary A. Morris[6], Roeland Van Malderen[7], Bryan J. Johnson[8], Richard R. Querel[9], Henry B. Selkirk[10,2], Rene Stübi[11], and Herman G. J. Smit[12]

[1]Earth System Science Interdisciplinary Center, University of Maryland, College Park, MD, USA

[2]Atmospheric Chemistry and Dynamics Lab, NASA/GSFC, Greenbelt, MD, USA

*Now at National Center for Atmospheric Research Earth Observations Laboratory, Boulder, CO, USA

[3]Science Systems and Applications, Inc., Lanham, MD, USA

[4]Environment and Climate Change Canada, Downsview, ON, CA

[5]National Center for Atmospheric Research Earth Observations Laboratory, Boulder, CO, USA

[6]St. Edwards University, Austin, TX, USA

[7]Royal Meteorological Institute of Belgium, Uccle (Brussels), Belgium

[8]Global Monitoring Division, NOAA Earth System Research Laboratory, Boulder, CO, USA

[9]National Institute of Water & Atmospheric Research (NIWA), Lauder, NZ

[10]Universities Space Research Association, Columbia, MD, USA

[11]Federal Office of Meteorology and Climatology, MeteoSwiss, Aerological Station, Payerne, Switzerland

[12]Institute of Chemistry and Dynamics of the Geosphere: Troposphere, Jülich Research Centre, Jülich, Germany

Contents of this file

Figures S1 to S6

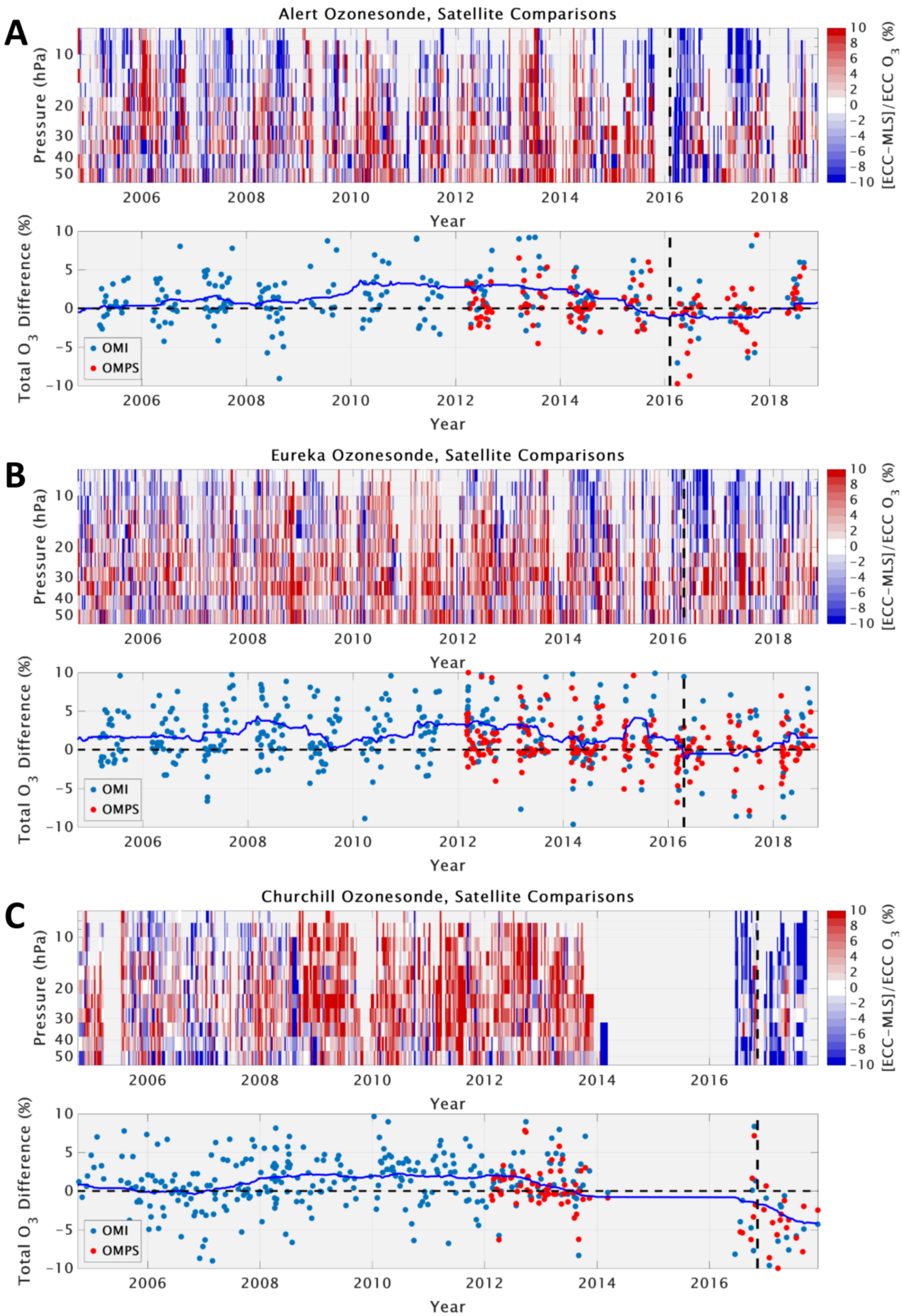
A
Alert Ozonesonde, Satellite Comparisons
Pressure (hPa)
[ECC−MLS]/ECC O3 (%)
Year
Total O3 Difference (%)
OMI
OMPS
B
Eureka Ozonesonde, Satellite Comparisons
Pressure (hPa)
[ECC−MLS]/ECC O3 (%)
Year
Total O3 Difference (%)
OMI
OMPS
C
Churchill Ozonesonde, Satellite Comparisons
Pressure (hPa)
[ECC−MLS]/ECC O3 (%)
Year
Total O3 Difference (%)
OMI
OMPS

D

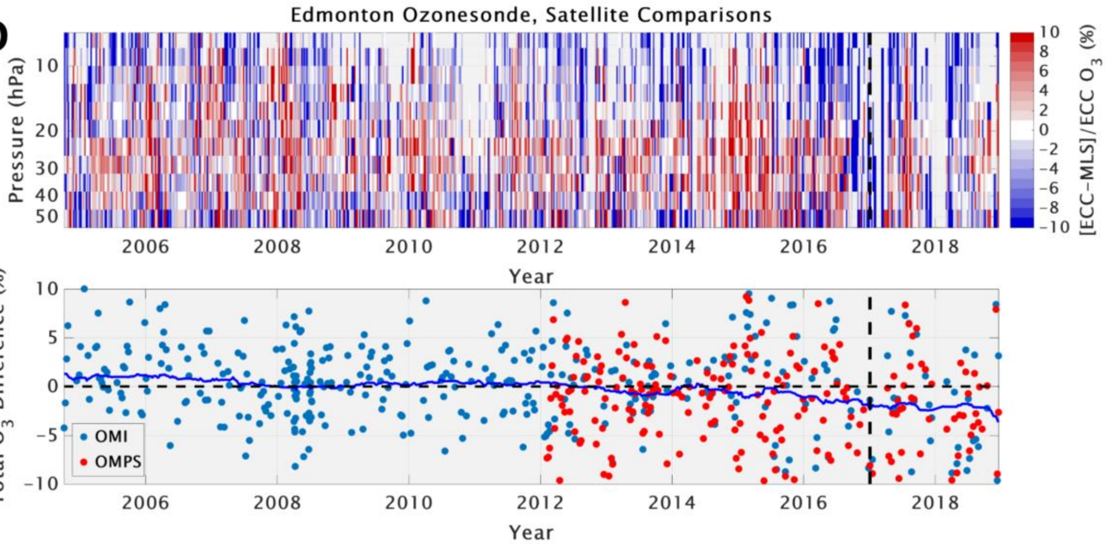
Edmonton Ozonesonde, Satellite Comparisons
Pressure (hPa)
[ECC−MLS]/ECC O_3 (%)
Year
Total O_3 Difference (%)
OMI
OMPS
Year

E

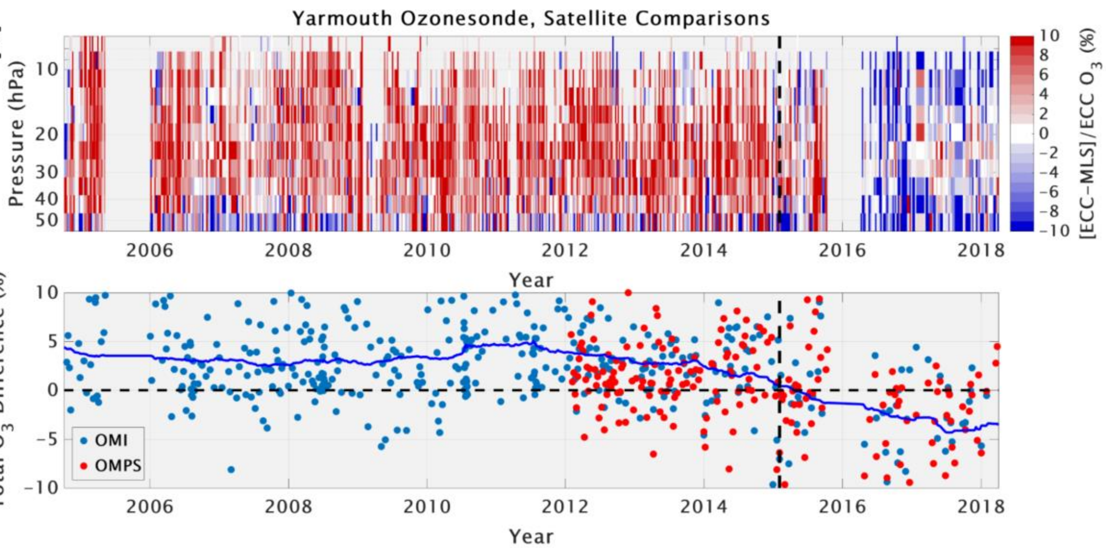
Yarmouth Ozonesonde, Satellite Comparisons
Pressure (hPa)
[ECC−MLS]/ECC O_3 (%)
Year
Total O_3 Difference (%)
OMI
OMPS
Year

F

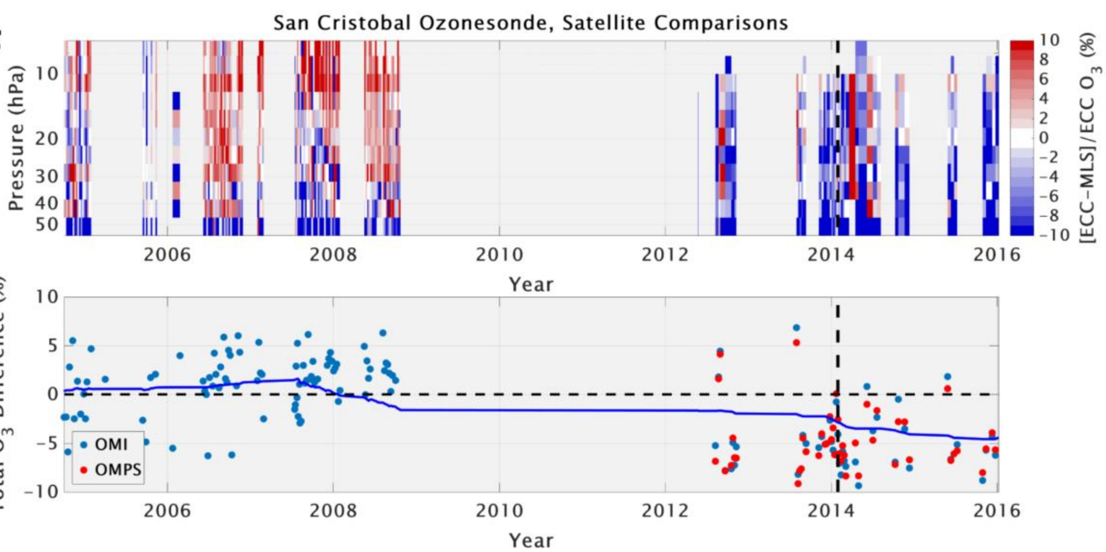
San Cristobal Ozonesonde, Satellite Comparisons
Pressure (hPa)
[ECC−MLS]/ECC O_3 (%)
Year
Total O_3 Difference (%)
OMI
OMPS
Year

G

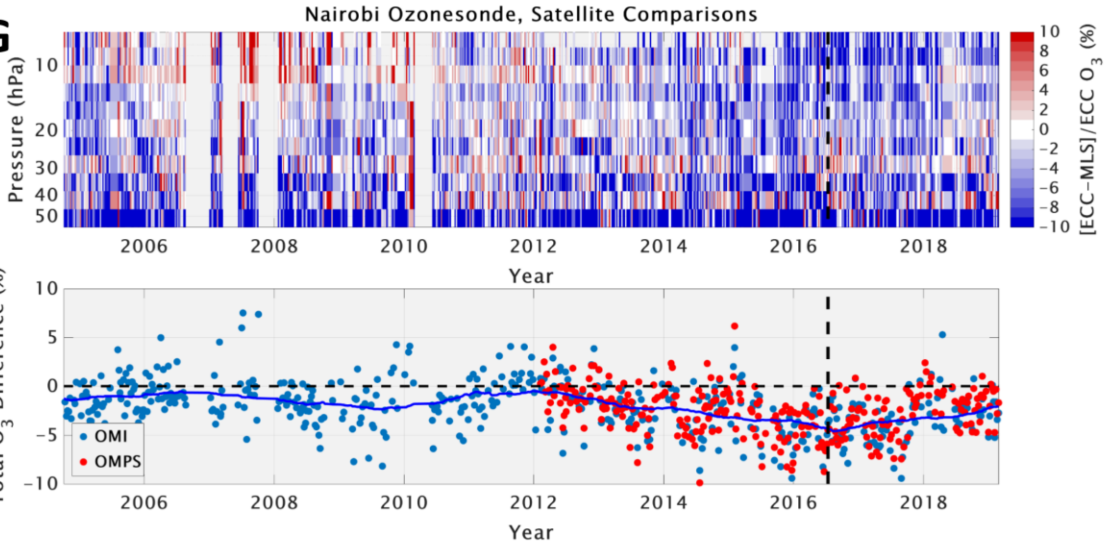
Nairobi Ozonesonde, Satellite Comparisons
Pressure (hPa)
[ECC−MLS]/ECC O3 (%)
Year
Total O3 Difference (%)
OMI
OMPS

H

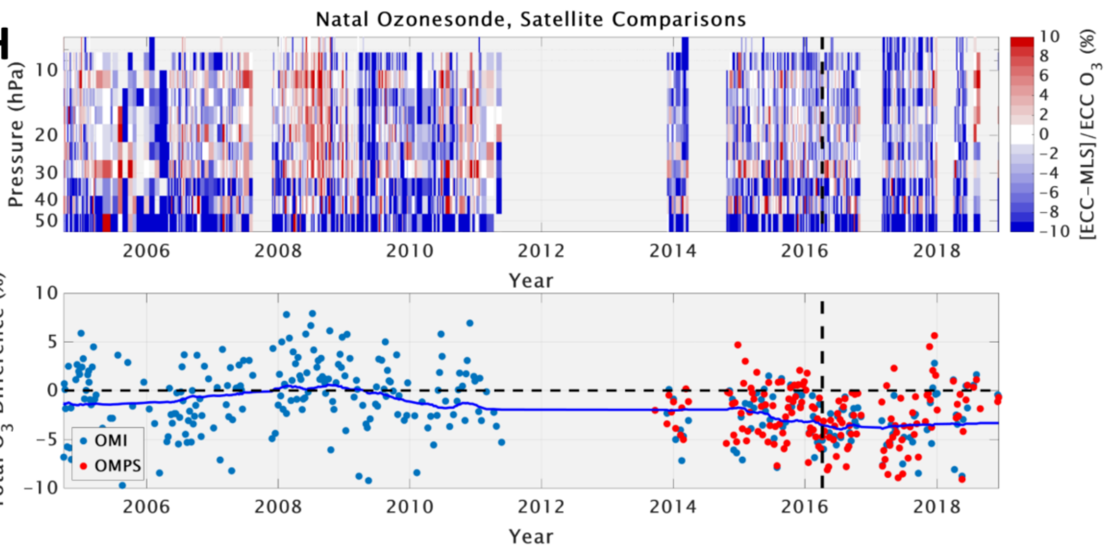
Natal Ozonesonde, Satellite Comparisons
Pressure (hPa)
[ECC−MLS]/ECC O3 (%)
Year
Total O3 Difference (%)
OMI
OMPS

I

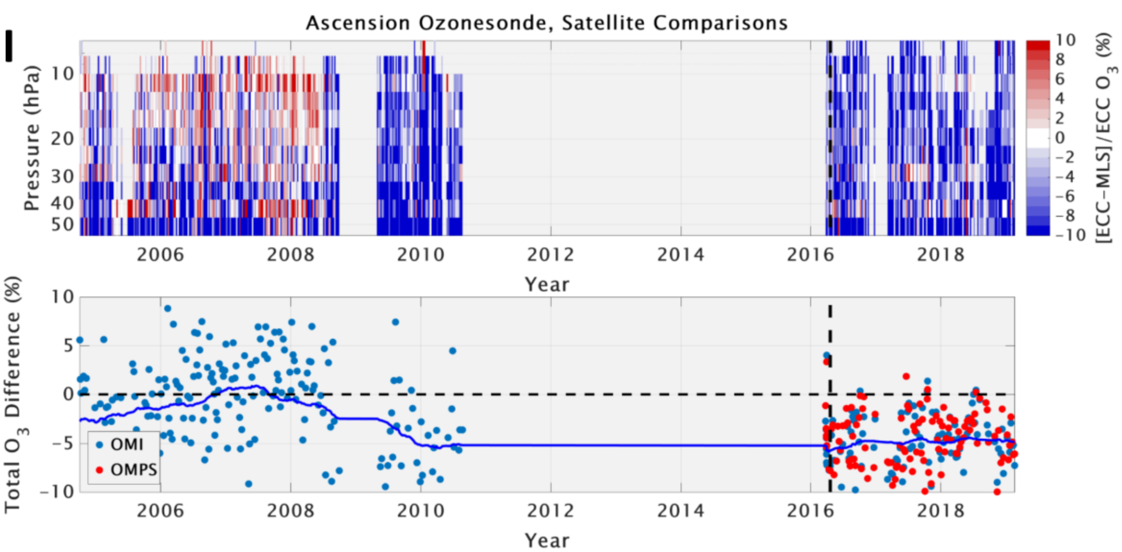
Ascension Ozonesonde, Satellite Comparisons
Pressure (hPa)
[ECC−MLS]/ECC O3 (%)
Year
Total O3 Difference (%)
OMI
OMPS

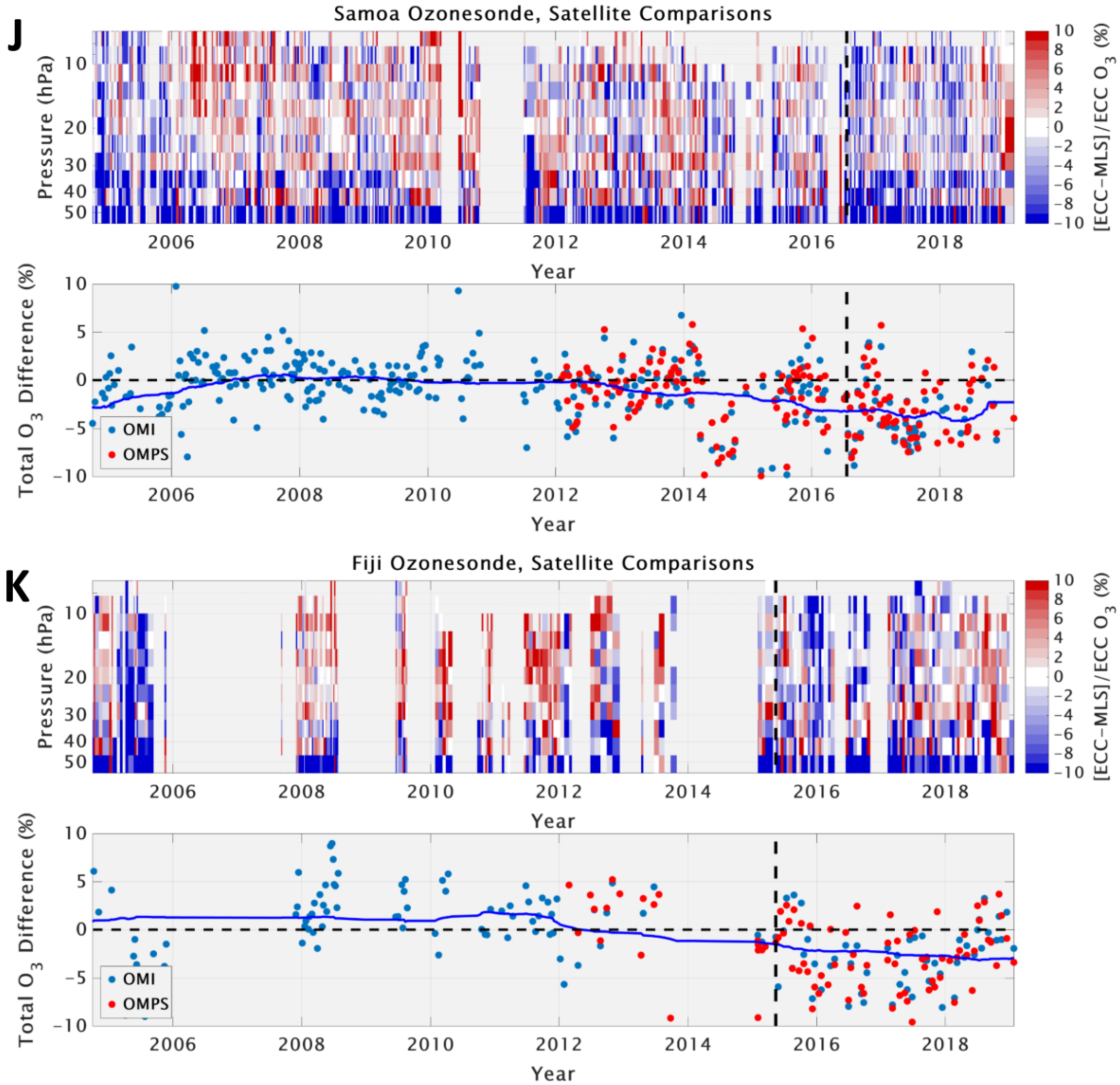

Figure S1. As in Figure 1, but for the 11 remaining affected ECC ozonesonde sites that exhibit a > 3 % drop-off in TCO relative to OMI. Note that the only affected Type2 station is Natal, Brazil (h). See Table 1 for more metadata on each site.

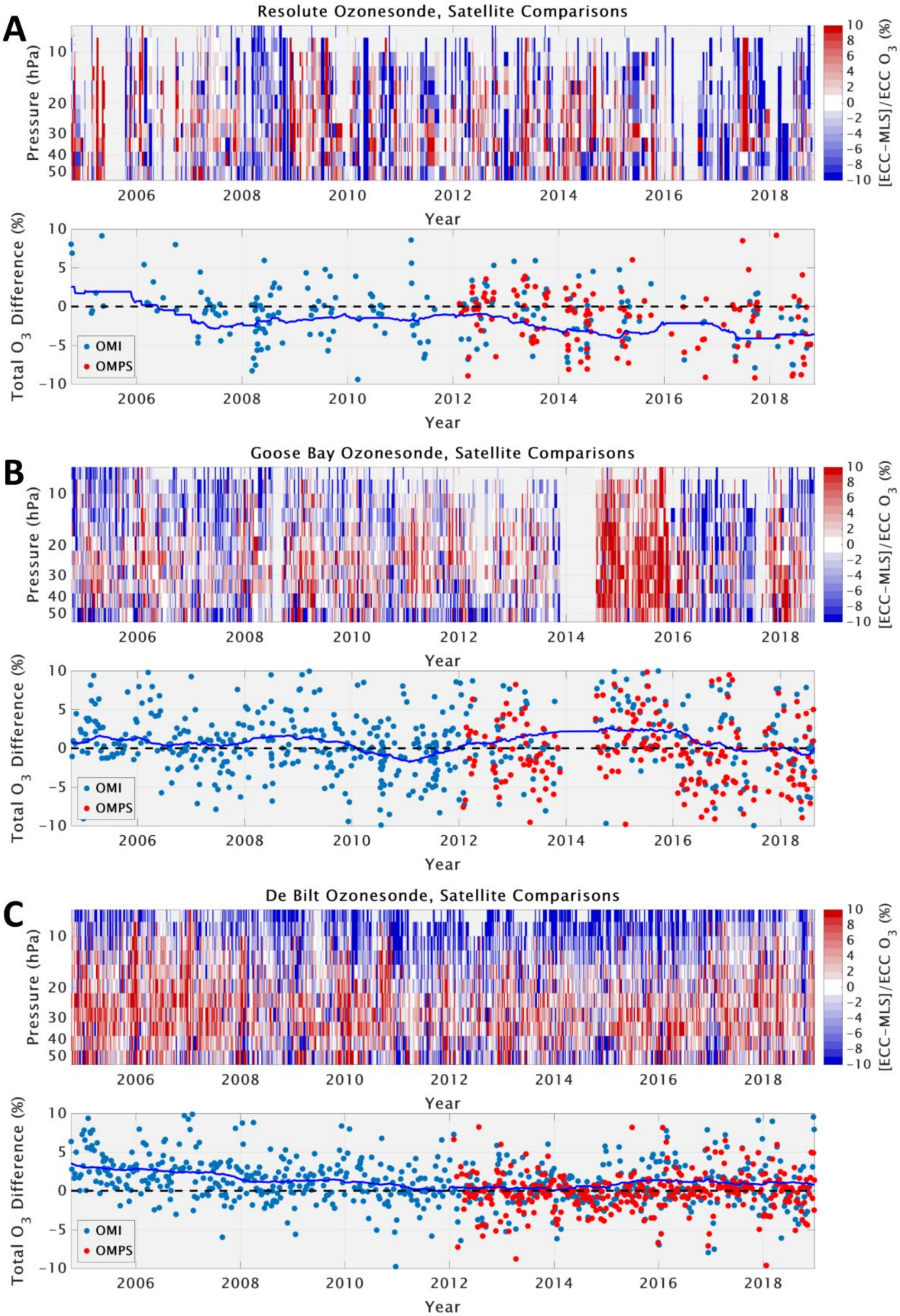

A
Resolute Ozonesonde, Satellite Comparisons
Pressure (hPa)
[ECC−MLS]/ECC O3 (%)
Year
Total O3 Difference (%)
OMI
OMPS
B
Goose Bay Ozonesonde, Satellite Comparisons
C
De Bilt Ozonesonde, Satellite Comparisons

D

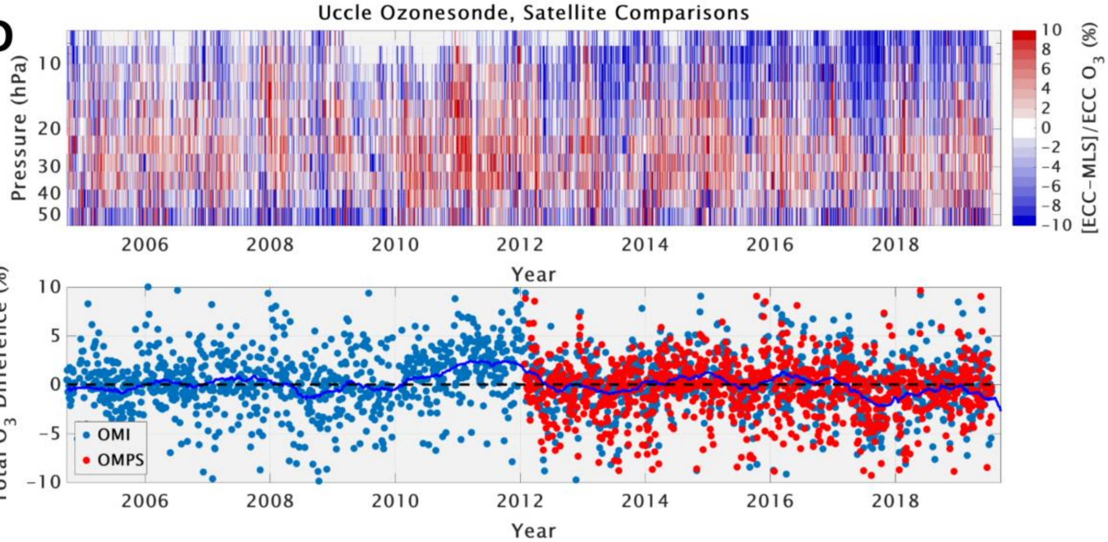
Uccle Ozonesonde, Satellite Comparisons
Pressure (hPa)
10
20
30
40
50
2006
2008
2010
2012
2014
2016
2018
Year
[ECC−MLS]/ECC O_3 (%)
10
8
6
4
2
0
−2
−4
−6
−8
−10
Total O_3 Difference (%)
OMI
OMPS
Year

E

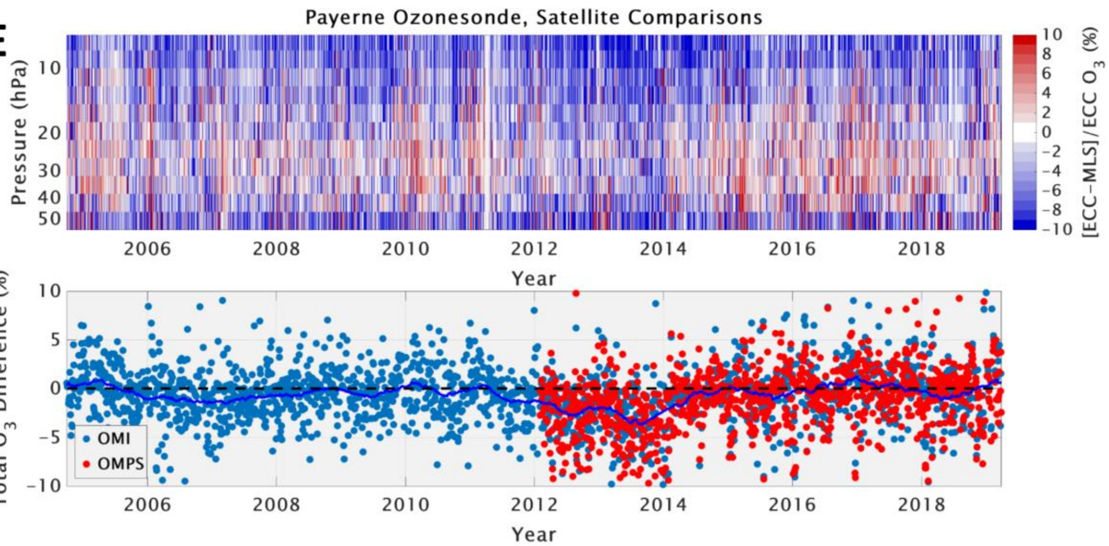
Payerne Ozonesonde, Satellite Comparisons
Pressure (hPa)
10
20
30
40
50
2006
2008
2010
2012
2014
2016
2018
Year
[ECC−MLS]/ECC O_3 (%)
Total O_3 Difference (%)
OMI
OMPS
Year

F

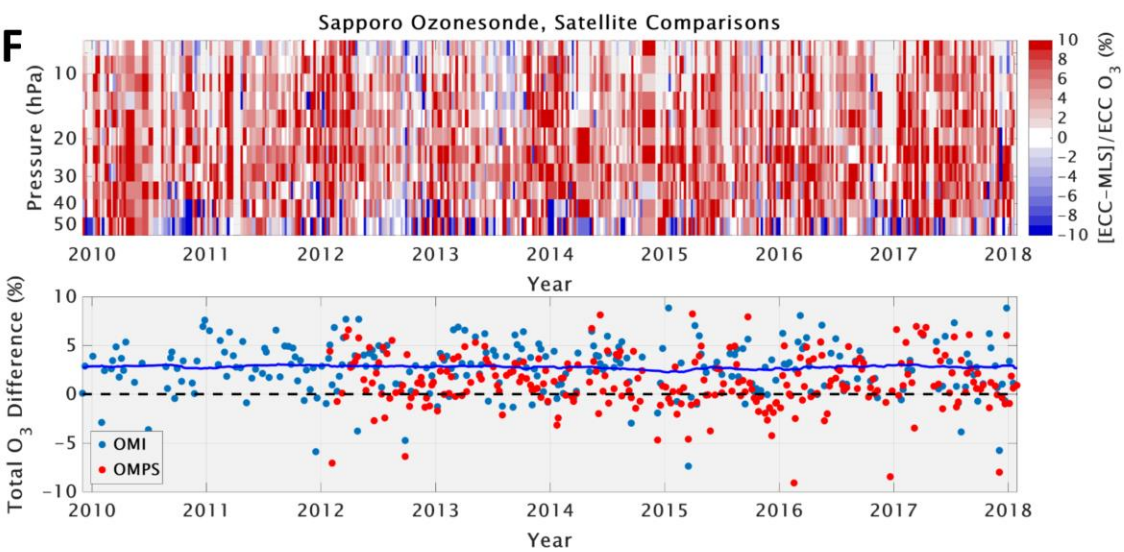
Sapporo Ozonesonde, Satellite Comparisons
Pressure (hPa)
10
20
30
40
50
2010
2011
2012
2013
2014
2015
2016
2017
2018
Year
[ECC−MLS]/ECC O_3 (%)
Total O_3 Difference (%)
OMI
OMPS
Year

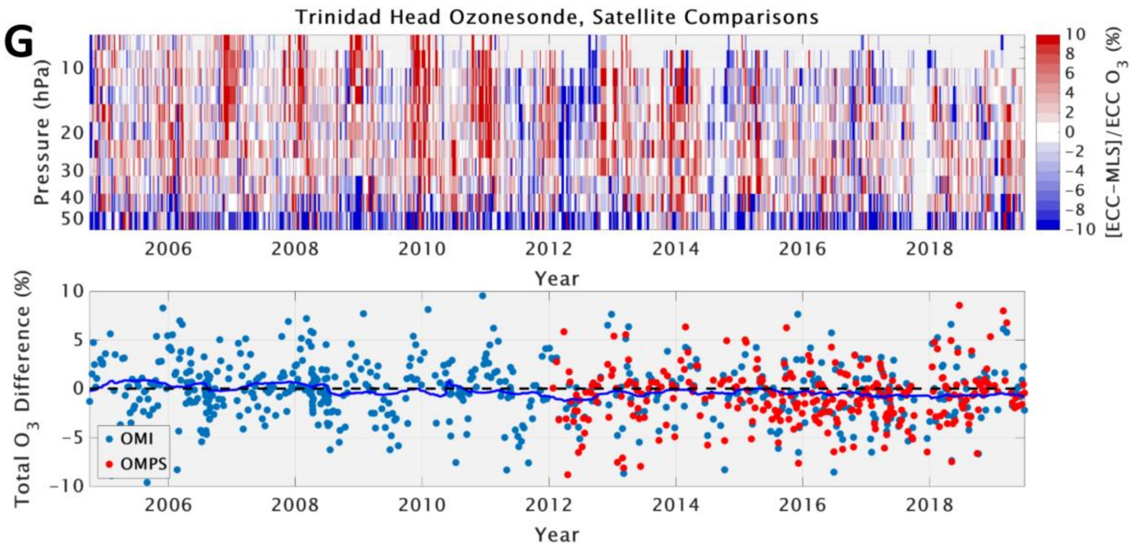
G
Trinidad Head Ozonesonde, Satellite Comparisons
Pressure (hPa)
[ECC−MLS]/ECC O_3 (%)
Year
Total O_3 Difference (%)
OMI
OMPS
Year

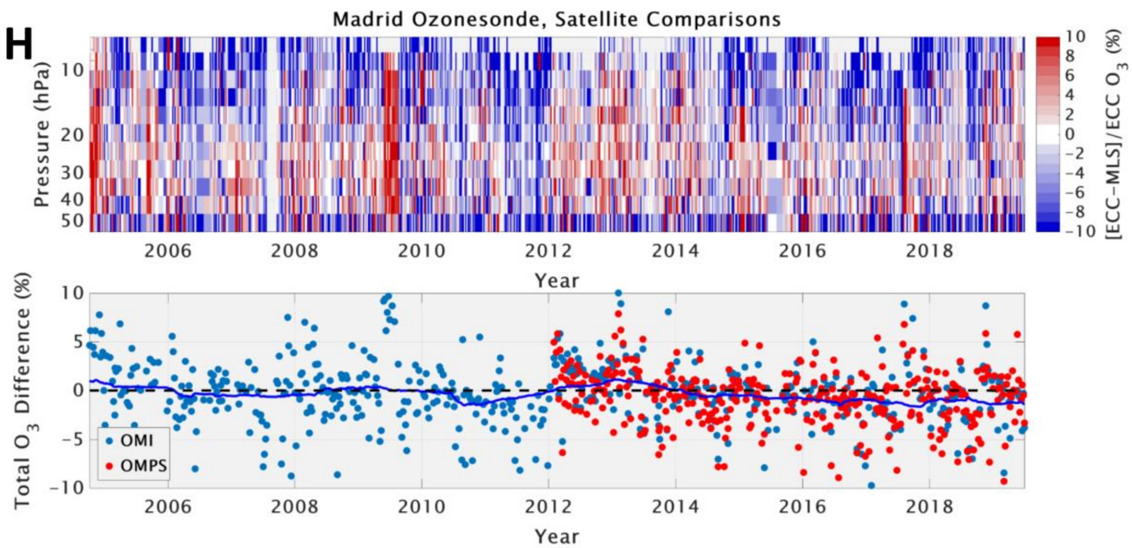
H
Madrid Ozonesonde, Satellite Comparisons
Pressure (hPa)
[ECC−MLS]/ECC O_3 (%)
Year
Total O_3 Difference (%)
OMI
OMPS
Year

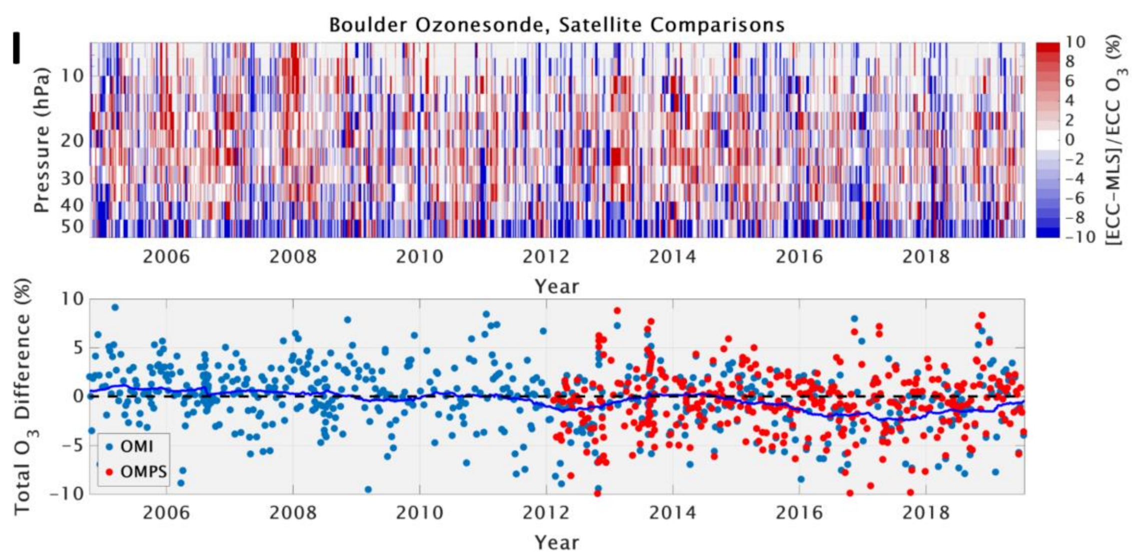
I
Boulder Ozonesonde, Satellite Comparisons
Pressure (hPa)
[ECC−MLS]/ECC O_3 (%)
Year
Total O_3 Difference (%)
OMI
OMPS
Year

J

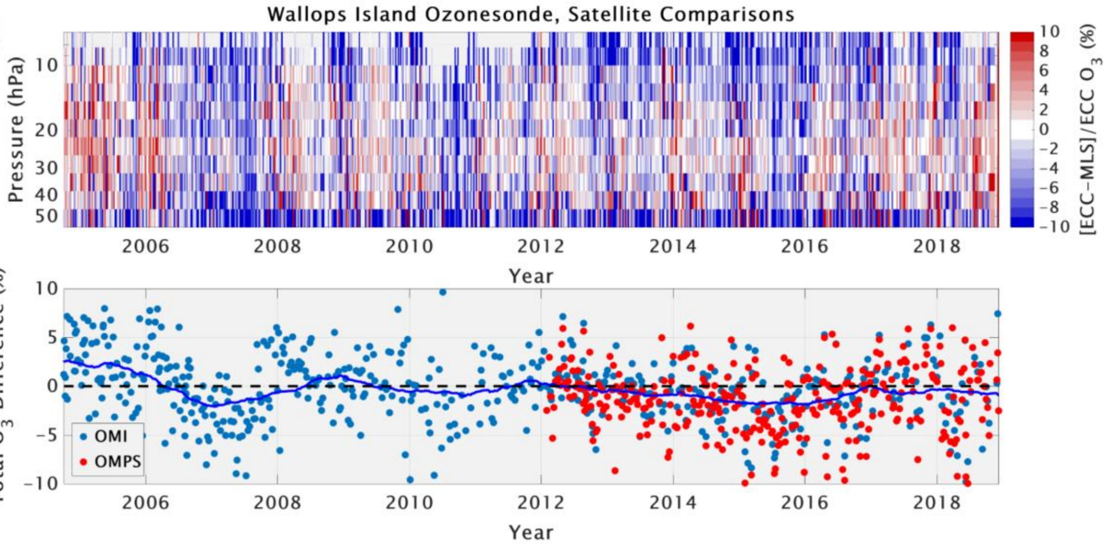
Wallops Island Ozonesonde, Satellite Comparisons
Pressure (hPa)
[ECC−MLS]/ECC O_3 (%)
Year
Total O_3 Difference (%)
OMI
OMPS
Year

K

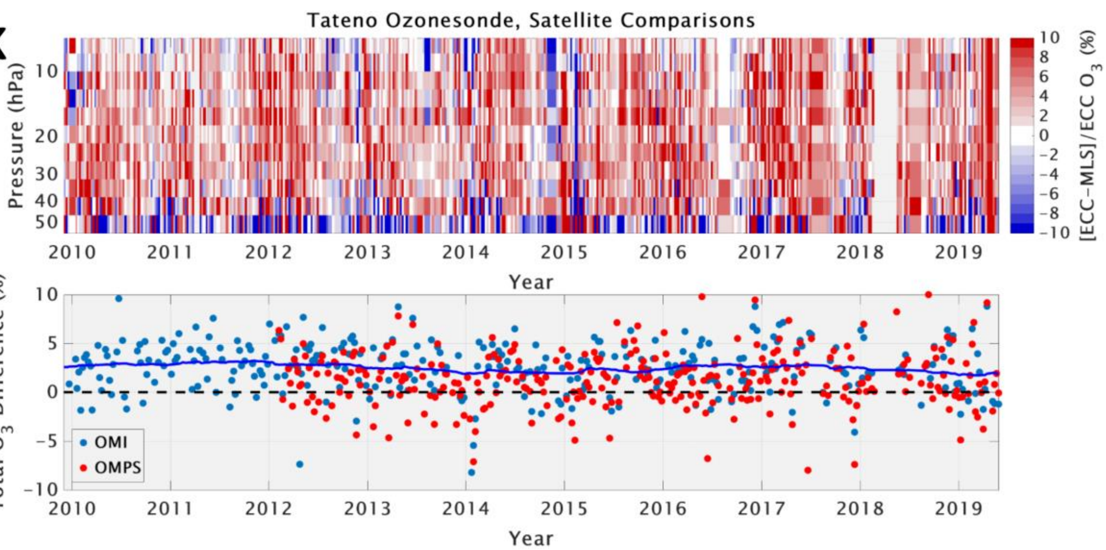
Tateno Ozonesonde, Satellite Comparisons
Pressure (hPa)
[ECC−MLS]/ECC O_3 (%)
Year
Total O_3 Difference (%)
OMI
OMPS
Year

L

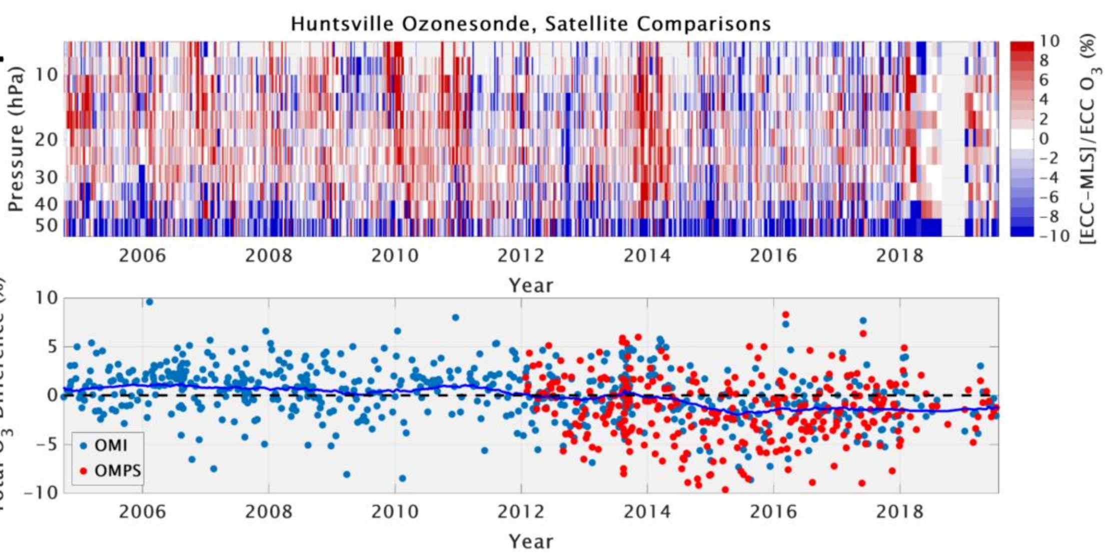
Huntsville Ozonesonde, Satellite Comparisons
Pressure (hPa)
[ECC−MLS]/ECC O_3 (%)
Year
Total O_3 Difference (%)
OMI
OMPS
Year

M

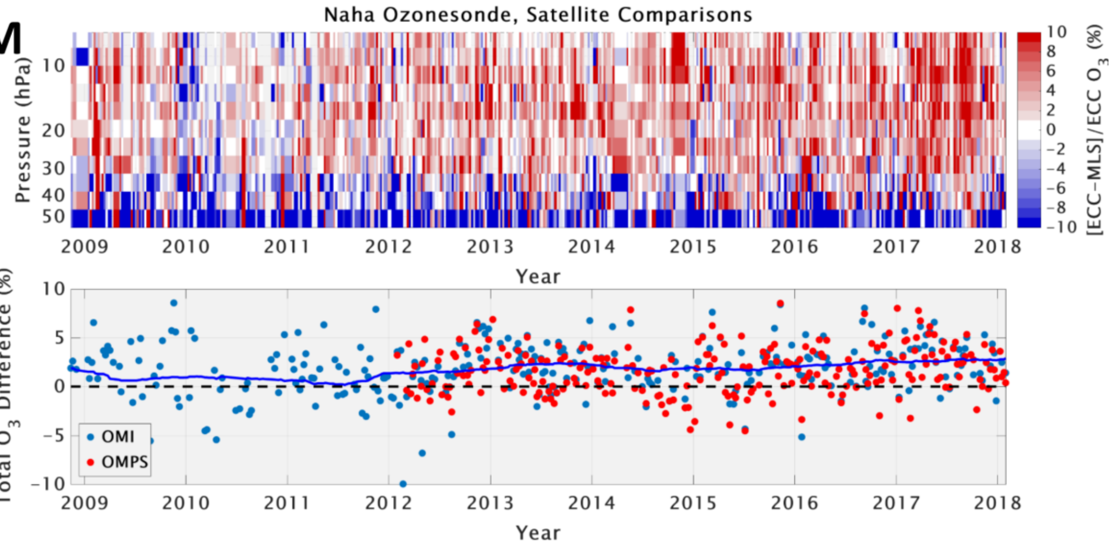
Naha Ozonesonde, Satellite Comparisons
Pressure (hPa)
[ECC−MLS]/ECC O3 (%)
Year
Total O3 Difference (%)
OMI
OMPS
Year

N

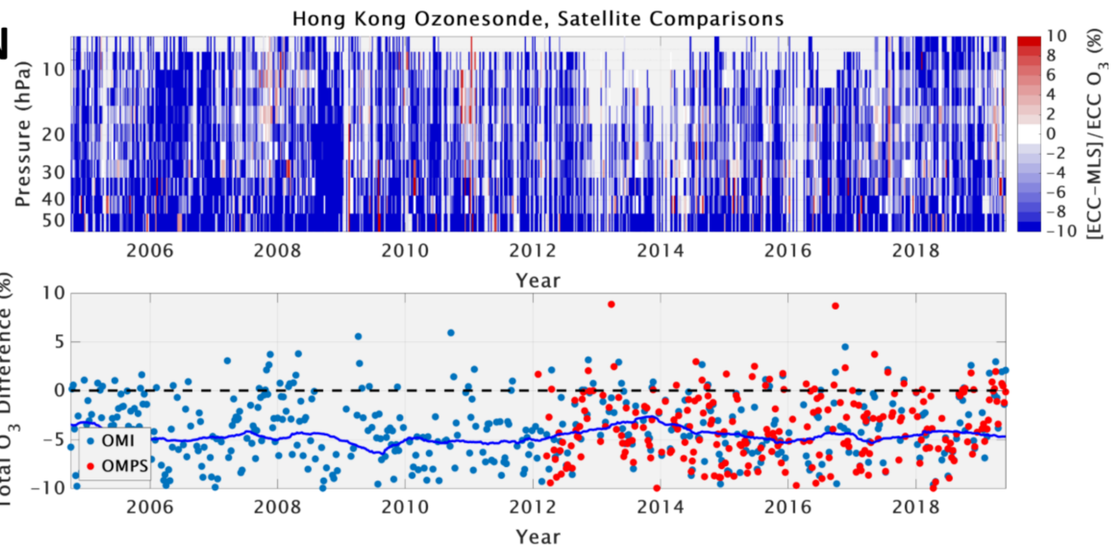
Hong Kong Ozonesonde, Satellite Comparisons
Pressure (hPa)
[ECC−MLS]/ECC O3 (%)
Year
Total O3 Difference (%)
OMI
OMPS
Year

O

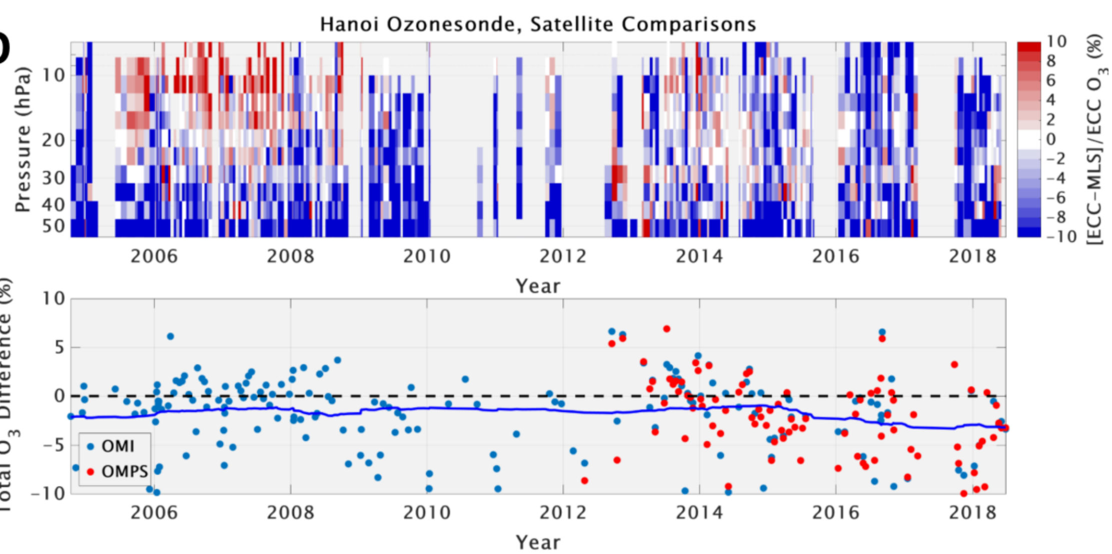
Hanoi Ozonesonde, Satellite Comparisons
Pressure (hPa)
[ECC−MLS]/ECC O3 (%)
Year
Total O3 Difference (%)
OMI
OMPS
Year

P

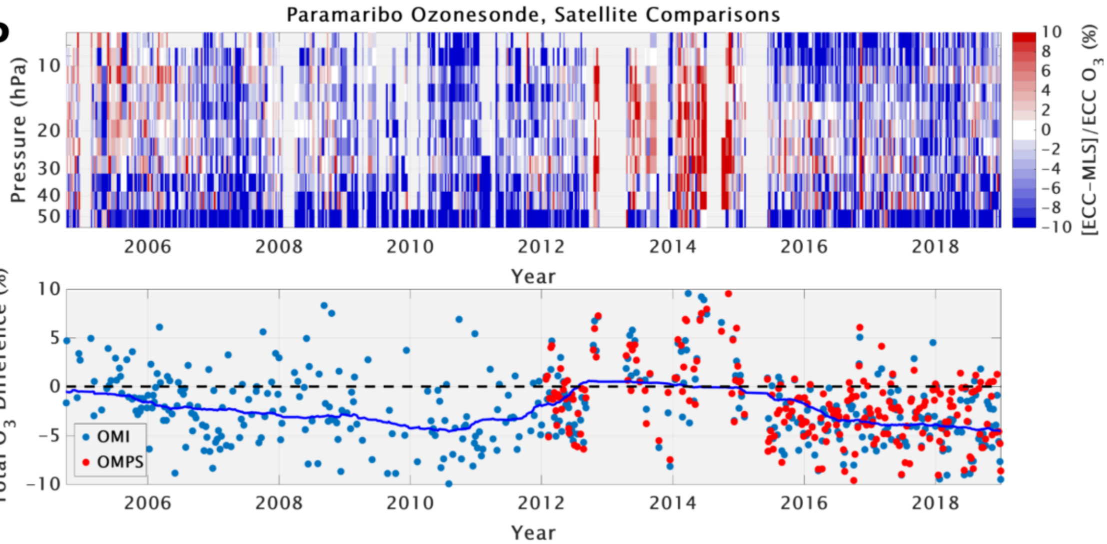
Paramaribo Ozonesonde, Satellite Comparisons
Pressure (hPa)
[ECC−MLS]/ECC O3 (%)
Year
Total O3 Difference (%)
OMI
OMPS
Year

Q

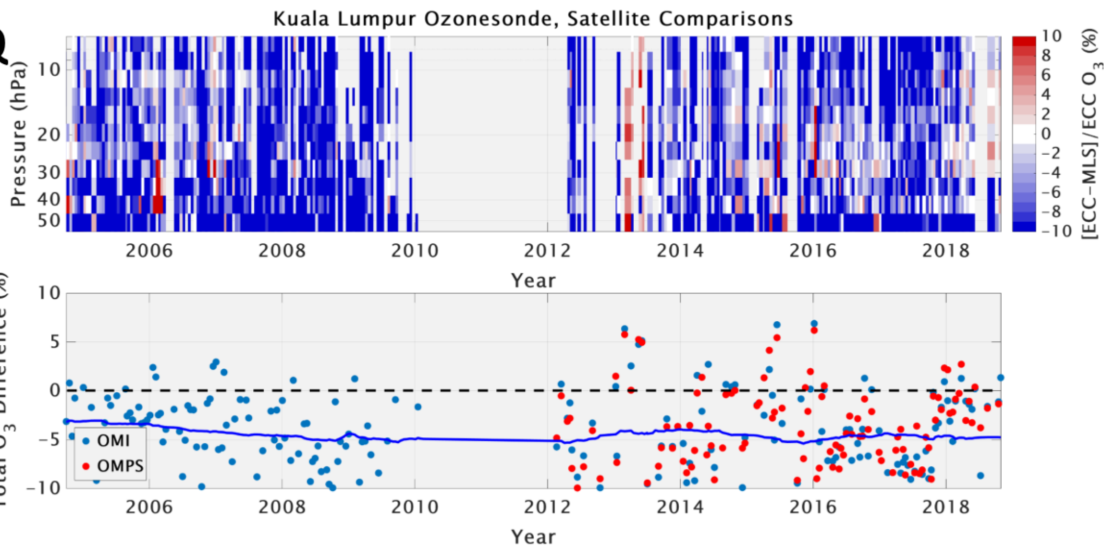
Kuala Lumpur Ozonesonde, Satellite Comparisons
Pressure (hPa)
[ECC−MLS]/ECC O3 (%)
Year
Total O3 Difference (%)
OMI
OMPS
Year

R

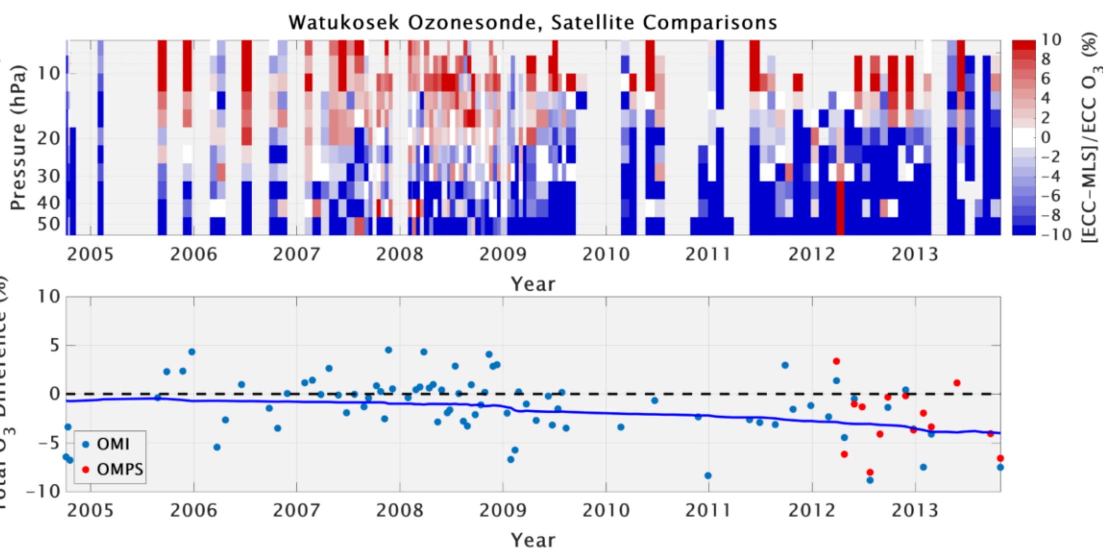
Watukosek Ozonesonde, Satellite Comparisons
Pressure (hPa)
[ECC−MLS]/ECC O3 (%)
Year
Total O3 Difference (%)
OMI
OMPS
Year

S

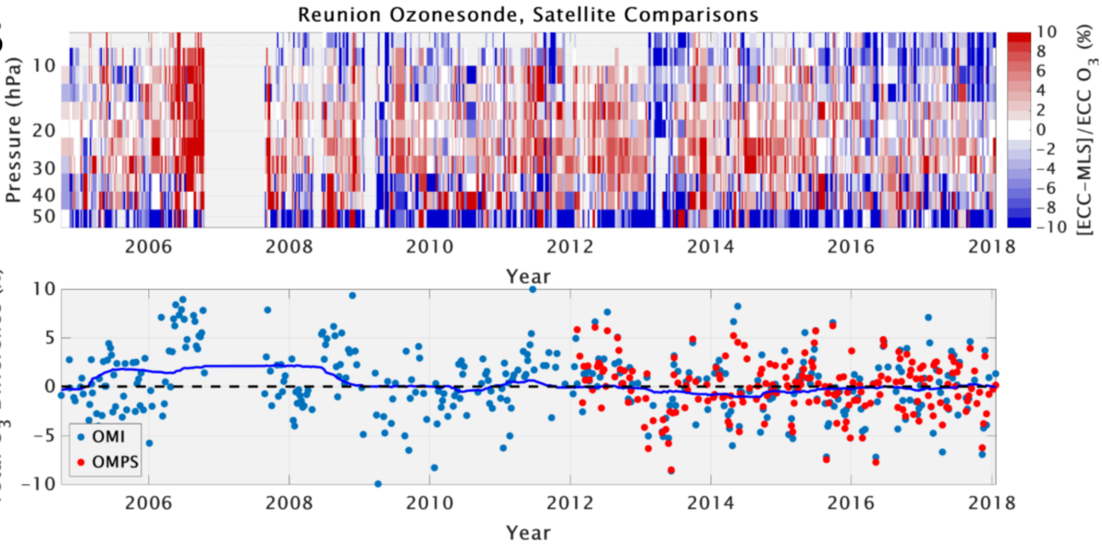
Reunion Ozonesonde, Satellite Comparisons
Pressure (hPa)
[ECC−MLS]/ECC O3 (%)
Year
Total O3 Difference (%)
OMI
OMPS

T

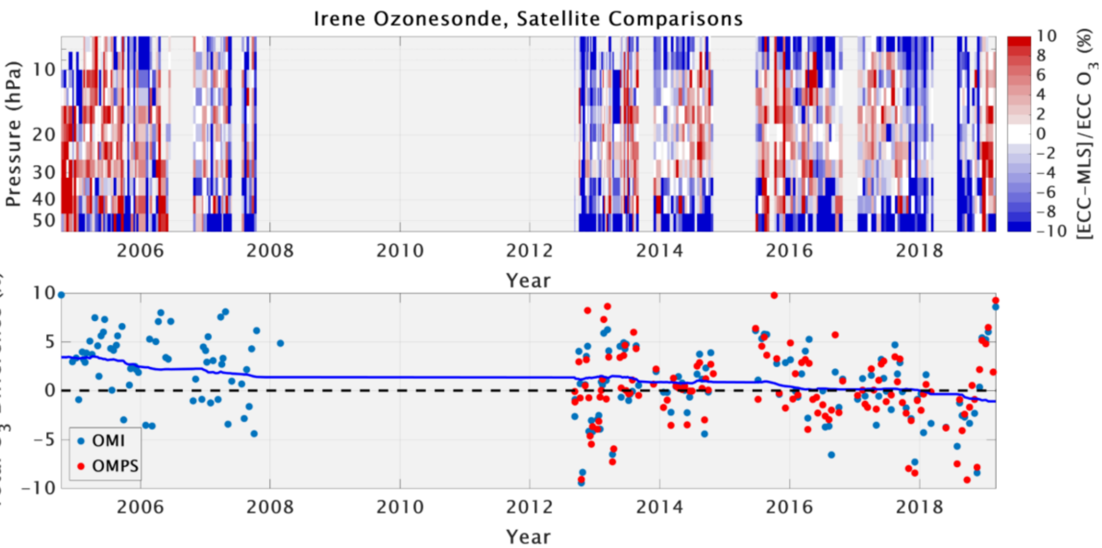
Irene Ozonesonde, Satellite Comparisons
Pressure (hPa)
[ECC−MLS]/ECC O3 (%)
Year
Total O3 Difference (%)
OMI
OMPS

U

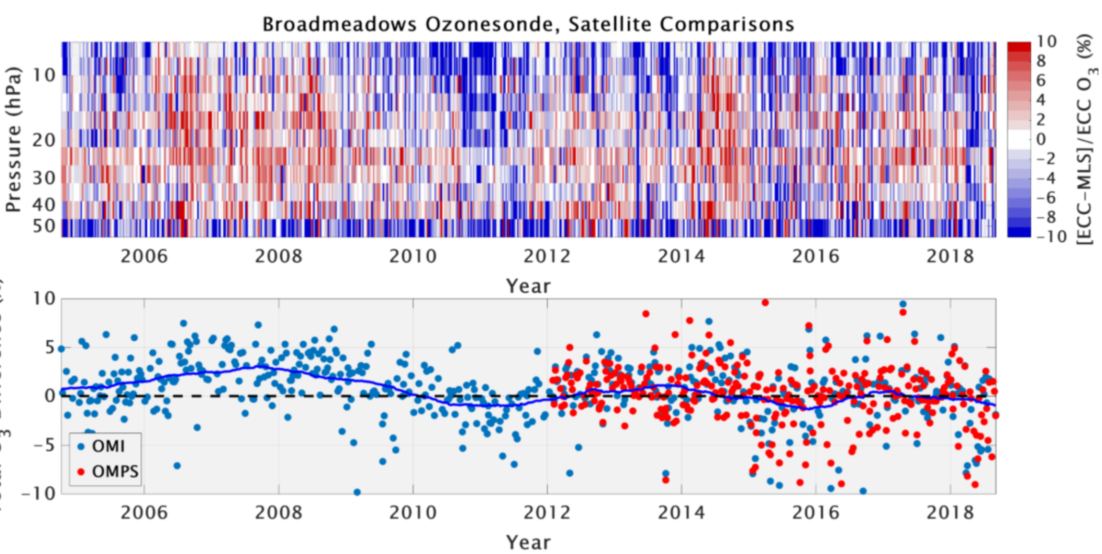
Broadmeadows Ozonesonde, Satellite Comparisons
Pressure (hPa)
[ECC−MLS]/ECC O3 (%)
Year
Total O3 Difference (%)
OMI
OMPS

V

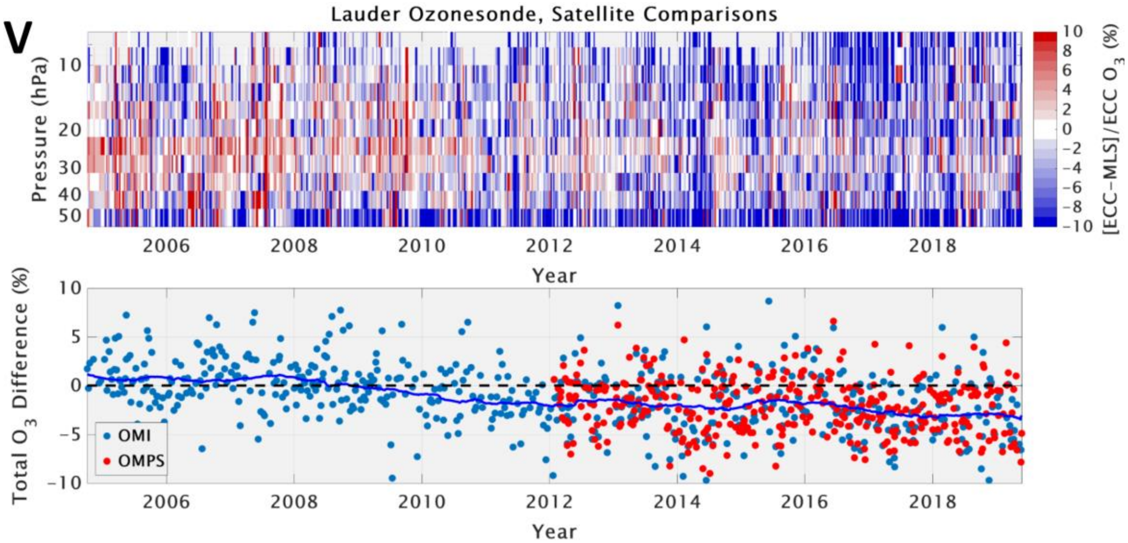

W

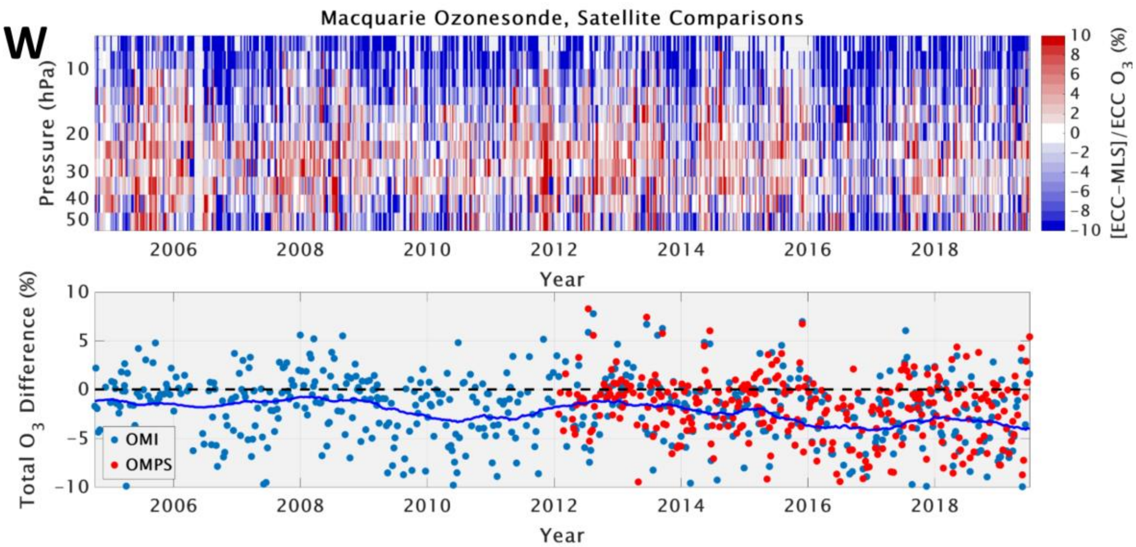

Figure S2. As in Figure 1, but for the 23 reference ECC ozonesonde sites (i.e. those that do not exhibit a > 3 % drop-off in TCO relative to OMI). See Table 1 for more metadata on each site.

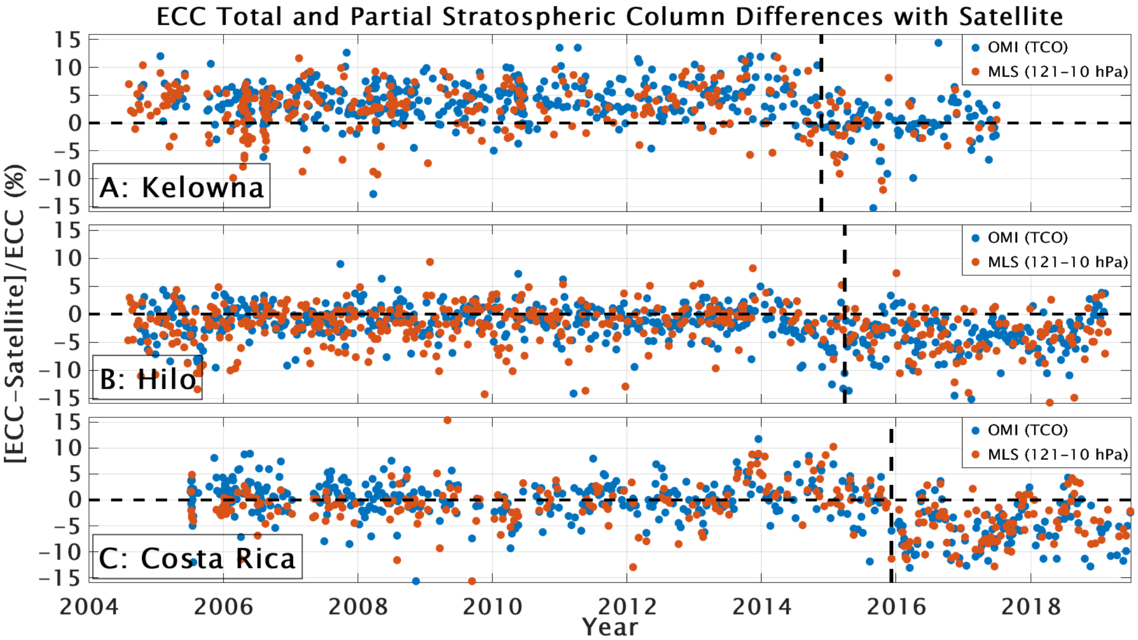

Figure S3. Time series of percent differences between ECC and OMI TCO (blue dots) and ECC and MLS partial stratospheric column O_3 integrated from 121 to 10 hPa (orange dots) for Kelowna (A), Hilo (B), and Costa Rica (C; the same sites as Figure 1). This shows the coincidence in the ECC stratospheric column drop vs. MLS with the TCO drop vs. OMI. The horizontal black dashed lines indicate the 0 % line and the vertical dashed lines indicate the date of ECC TCO drop-off (see Table 1).

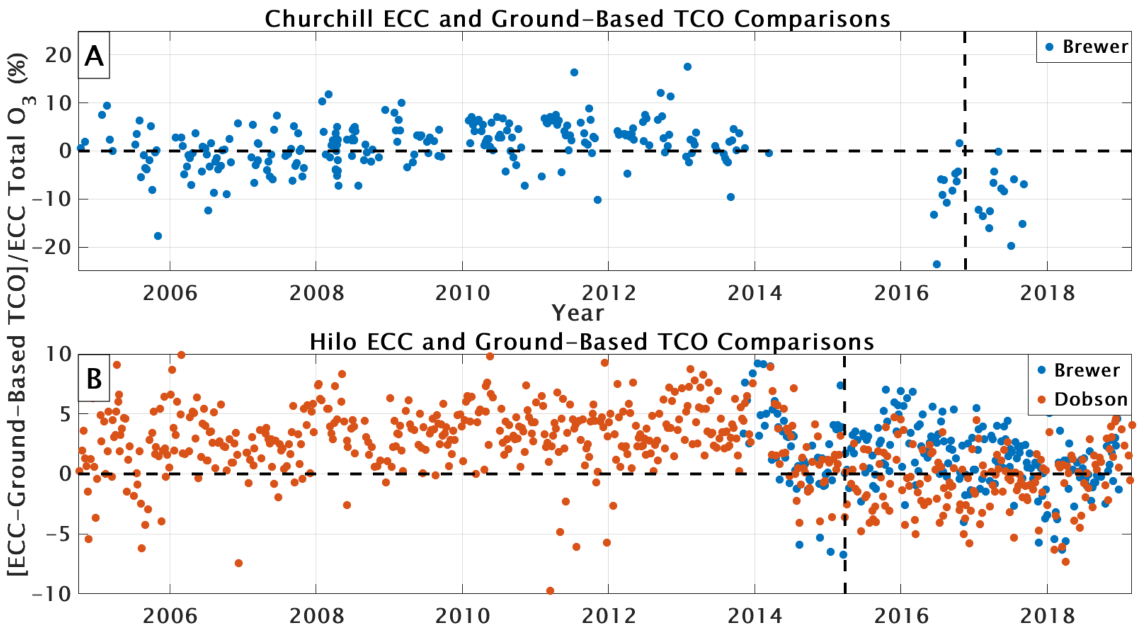

Figure S4. Time series of comparisons between ECC and ground-based TCO measurements at Churchill, Canada (A), and Hilo, HI (B). Horizontal dashed lines indicate the 0 % line for TCO comparisons, and the vertical black dashed lines indicate the date of ECC drop-off (see Table 1). Note the different y-scales for each panel.

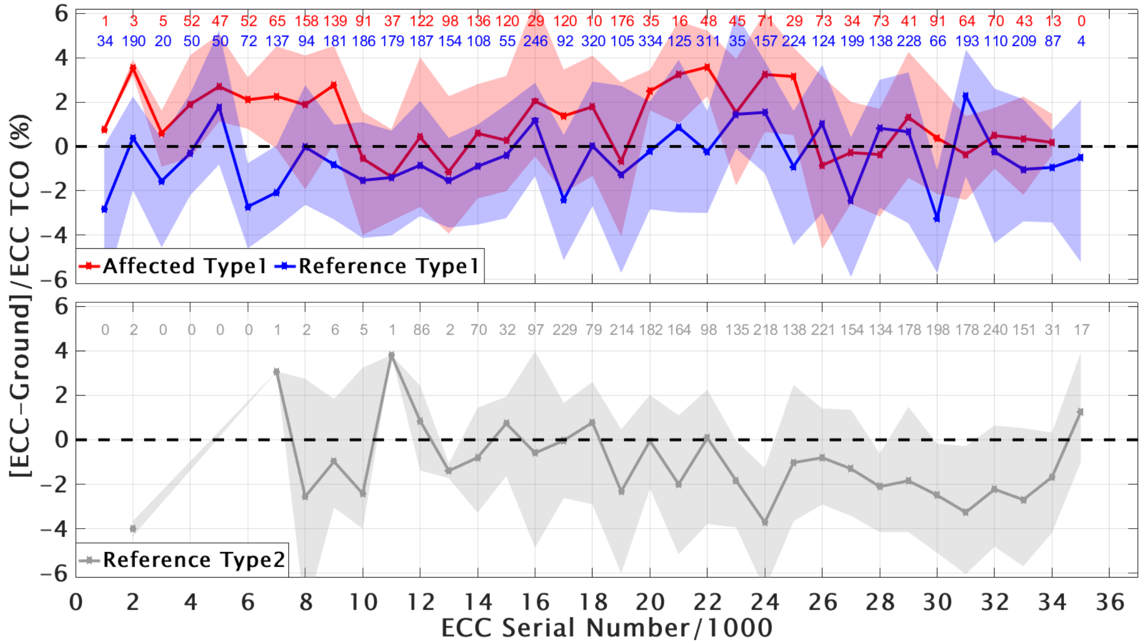

Figure S5. Median (lines) and 25th to 75th (shading) percentiles of comparisons between ECC and ground-based TCO. The comparisons are separated by every 1000 serial numbers for Type1 (top) and Type2 (bottom) ECCs. The Type1 ECCs are separated into affected (red; six available sites) and reference (blue; nine sites) stations. Natal, the only affected Type2 site, is not included in this figure, leaving seven Type2 sites that have available ground-based data for this comparison (Hong Kong does not have ground-based TCO data available). The number of samples for each serial number bin are shown at the top of each panel.

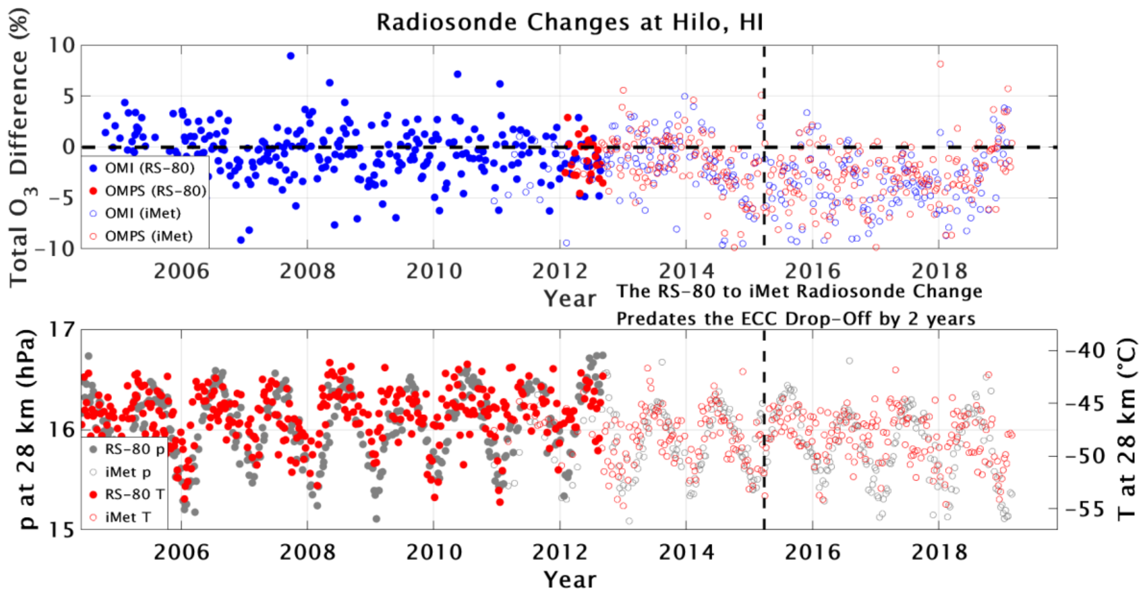

Figure S6. Top panel: Time series of TCO percent differences between Hilo ECC, and OMI (blue) and OMPS (red) TCO. Bottom panel: Pressure (grey) and temperature (red) values at 28 km altitude (representative of the mid-stratosphere). The solid dots show when the ECC ozonesonde was paired with a Vaisala RS-80 radiosonde, and the open dots show when the ECC was paired with an InterMet iMet radiosonde. The vertical dashed lines indicate the date of the ECC TCO drop-off at Hilo (see Table 1), and the horizontal line on the top panel indicates the 0 % line for TCO comparisons.